

Aus dem Pathologischen Institut,
Institut der Ludwig-Maximilians Universität
München
Vorstand: Prof. Dr. Frederick Klauschen

**Belizatinib is a potent inhibitor for non-small cell
lung cancers driven by different variants of EML4-
ALK fusion proteins carrying L1196M-mutations**

Dissertation
zum Erwerb des Doktorgrades der Medizin an der
Medizinischen Fakultät der
Ludwig-Maximilians-Universität zu München

vorgelegt von

Pan LI

aus

Hubei, P.R.China

2022

Mit Genehmigung der Medizinischen Fakultät
der Universität München

Berichterstatter:	Prof. Dr. Andreas Jung
Mitberichterstatter:	Prof. Dr. Roland Kappler Prof. Dr. Claus Belka PD Dr. Amanda Tufman
Mitbetreuung durch den promovierten Mitarbeiter:	Dr. Jörg Kumbrink
Dekan:	Prof. Dr. med. Thomas Gudermann
Tag der mündlichen Prüfung:	30.11.2022

Contents

Zusammenfassung (Deutsch):.....	1
Abstract (English):.....	2
List of figures.....	3
List of tables.....	4
List of abbreviations	5
1 Introduction	7
1.1 General diagnosis and treatment of Non-small cell lung cancer (NSCLC)	7
1.2 NSCLC is a paradigm of precision medicine	8
1.3 ALK rearrangements in NSCLC	10
1.3.1 ALK biology and oncogenesis	10
1.3.2 EML4-ALK fusion gene	11
1.4 Targeting EML4-ALK fusion genes	13
1.4.1 First-generation TKI– crizotinib.....	13
1.4.2 Second-generation TKIs- ceritinib, alectinib and brigatinib.....	14
1.4.3 Third-generation TKI —lorlatinib.....	15
1.4.4 Others.....	15
1.5 ALK-TKI resistance mechanisms	17
1.5.1 ALK-independent resistance.....	17
1.5.2 ALK-dependent resistance	18
2 Materials and methods	21
2.1 Materials.....	21
2.2 Methods.....	26
2.2.1 Information acquisition online	26
2.2.2 Mutagenesis.....	27
2.2.3 Gel electrophoresis	27
2.2.3 Colony PCR and sequencing	27
2.2.4 Plasmid DNA purification	28
2.2.5 Cell culture	29
2.2.6 Electroporation.....	30
2.2.7 IL3/blastidicin selection and cell cloning	31
2.2.8 Western blotting	31
2.2.9 Cell viability assay (IC50).....	32
2.2.10 Molecular docking	33
2.2.11 Data analysis and statistics	34
3 Results.....	35
3.1 Information collection of ALK-TKIs resistance spectra with corresponding mutations and fusion variants	35
3.2 Construction of expression plasmids encoding EML4-ALK fusion variants with resistance mutations.....	36
3.3 Selecting cell clonings with designed mutations and fusion variants.....	38
3.4 Dose selection and cell model reliability assessment	38
3.5 Activity of ALK-TKIs in different combinations of resistance mutations and fusion variants	40
3.6 Belizatinib is the most potent inhibitor of EML4-ALK fusion proteins with L1196M mutation.....	44
3.7 Increased compound–protein interaction (CPI) contribute to the sensitivity of ALK-L1196M to belizatinib	45
4 Discussion.....	48
5 References.....	53
6 Appendix A:	62
7 Appendix B:	63
8 Acknowledgments	64
9 Affidavit	65

Zusammenfassung (Deutsch):

Strukturelle Fusionen von EML4 mit der ALK-Kinase führen zu Signalanomalien, die NSCLC verursachen. Obwohl zugelassene spezifische ALK-Inhibitoren bei ALK-positiven NSCLC-Patienten zu einem ausgezeichneten anfänglichen Ansprechen geführt haben, stellen erworbene Resistenzen gegen diese Inhibitoren aufgrund des Auftretens von Mutationen eine große klinische Herausforderung dar. Studien haben gezeigt, dass verschiedene Mutationen mit einzigartigen und spezifischen Reaktionen auf bestimmte Inhibitoren verbunden sind, und dass die Empfindlichkeit von EML4-ALK-Fusionsvarianten (V) gegenüber ALK-spezifischen Inhibitoren variiert. Um das Ansprechspektrum von Kombinationen der einzelnen Resistenzmutationen und EML4-ALK-Fusionsgenvarianten auf verschiedene ALK-spezifische Inhibitoren zu untersuchen, wurden in dieser Studie individuelle zelluläre Ba/F3-Modelle konstruiert und für ein ALK-TKI-Screening eingesetzt. Auf der Grundlage von Zell-Überlebenstests legten die in dieser Arbeit gewonnenen Ergebnisse nahe, dass Brigatinib vorrangig für G1269A- und L1152R-Mutationen, Lorlatinib für C1156Y- und I1171T-Mutationen und Belizatinib für G1269A- und L1196M-Mutationen empfohlen werden könnten. Darüber hinaus wurde die Tendenz beobachtet, dass V2 am sensitivsten auf ALK-TKI reagierte, gefolgt von V1 und V3b. V3a zeigte die geringste Sensitivität. Es gab jedoch Situationen, in denen die Sensitivität gegenüber Medikamenten nicht mit den erwarteten additiven Effekten der mutations- und variantenabhängigen Sensitivität übereinstimmten, was auf die Notwendigkeit hinwies, sowohl Varianten als auch Mutationen gemeinsam zu berücksichtigen. Insbesondere Belizatinib, ein in der Entwicklung befindliches Medikament, war bei allen Arten von Fusionsvarianten etwa zwanzigmal so wirksam wie Lorlatinib gegen ALK-L1196M. Die vielversprechende Wirksamkeit von Belizatinib gegen die L1196M-Mutation von EML4-ALK wurde auch durch eine Simulation der Molekulardynamik bestätigt. Zusammenfassend wurden in dieser Arbeit ❶ Sensitivitätsspektren mit klinisch bestätigten EML4-ALK-Mutations-Fusions-Kombinationen für neun ALK-TKIs erarbeitet, ❷ eine mögliche optimale Abfolge von ALK-TKIs für die Behandlung ALK-positiver Patienten, die während der Therapie Resistenzmutationen entwickeln, aufgezeigt und ❸ Belizatinib als vielversprechenden möglichen gezielten Inhibitor für die L1196M-Mutation von EML4-ALK bei NSCLC gefunden.

Abstract (English):

Structural fusions of EML4 with ALK kinase might lead to signaling abnormalities that drive NSCLC. Although approved specific ALK inhibitors have led to excellent initial responses in ALK positive NSCLC patients, acquired resistance to these inhibitors due to the occurrence of mutations is a major clinical challenge. Studies have shown that different mutations are related with unique and specific responses to certain inhibitors, and that the sensitivity of EML4-ALK fusion variants to ALK specific inhibitors varies. To investigate the response spectrum of combinations of each resistance mutation and **EML4-ALK** fusion gene variant (V) to different ALK specific inhibitors, individual cellular Ba/F3 models were constructed and used for **ALK-TKIs** screening in this thesis. Based on cell viability assays, the results gained here suggested that brigatinib might be priority recommended for G1269A and L1152R mutations, lorlatinib for C1156Y and I1171T mutations and belizatinib for G1269A and L1196M mutation. Moreover, a tendency was observed that V2 was most sensitive to ALK-TKIs, V1 and V3b had intermediate sensitivity and V3a was the least sensitive. **But** there were situations where drug sensitivity was not in line with the expected additive effects of mutation- and variant- dependent sensitivities, which indicated the necessity of taking both variants and mutations into consideration. Notably, belizatinib, a drug in development, was approximately twenty times as potent as lorlatinib for **ALK-L1196M** in all types of fusion variants. The promising efficacy of belizatinib against L1196M mutation of EML4-ALK were also proven by molecular dynamics simulations. In conclusion, the results of this study ❶ provided sensitivity spectra with clinical confirmed EML4-ALK mutation-fusion combinations to nine ALK-TKIs, ❷ offered a possible optimal sequence of ALK-TKIs for treating ALK-positive patients developing resistance mutations during therapy and ❸ suggested belizatinib as a promising possible targeted inhibitor for the L1196M mutation of EML4-ALK in NSCLC.

List of figures

Figure 1 Biology and oncogenesis of the ALK oncogene.

Figure 2 Protein domain structures of EML4 and ALK and chromosomal rearrangement for EML4-ALK variants.

Figure 3 Structure of human wild type (WT) ALK kinase domain depicting domains and commonly found resistance mutations for ALK specific TKIs.

Figure 4 Cell viability of Ba/F3 cells with different concentration of IL3.

Figure 5 Construction and confirmation of point mutations conferring ALK-inhibitor resistance in expression plasmids containing EML4-ALK fusion variants.

Figure 6 ALK and pALK expression of different mutations in EML4-ALK variants.

Figure 7 Dose selection and cell model reliability assessment.

Figure 8 Inhibition efficacy of different ALK-TKIs against Ba/F3 cells harboring various EML4-ALK fusion variants and L1196M-, I1171T-, G1202R-, C1156Y-, G1269A- or L1152R mutations.

Figure 9 Effect of crizotinib, lorlatinib and belizatinib on ALK phosphorylation in different EML4-ALK fusion variants with L1196M mutation.

Figure 10 Predicted compound-protein interactions of belizatinib and ALK-WT or ALK-L1196M, respectively.

Figure 11 IC₅₀ of Ba/F3 cells harboring ALK-WT and ALK-L1196M by treatment with belizainib.

List of tables

Table 1 The *nationale Netzwerk Genomische Medizin* (nNGM) diagnostic panel for NSCLC.

Table 2 EML4-ALK variants and their properties.

Table 3 EMA-approved and unapproved ALK inhibitors used in this study.

Table 4 Individual responses to ALK inhibitors reported with corresponding ALK-gene mutation and EML4 fusion variant information.

Table 5 Mean IC₅₀ (nM) of ALK-TKIs on cellular ALK phosphorylation in Ba/F3 cells harboring EML4-ALK variants with C1156Y, L1196M, G1269A, I1171T, L1152R and G1202R mutations.

Table 6 Computational simulation of the binding affinity of crizotinib, lorlatinib and belizatinib to ALK-WT and ALK-L1196M and average IC₅₀ values of cell models.

List of abbreviations

ALEC	alectinib
ALK	anaplastic lymphoma kinase
AUC	areas under ROC curves
BELI	belizatinib
BRIG	brigatinib
CEP	CEP-37440
CERT	ceritinib
CKB	The Clinical Knowledgebase
CIViC	clinical interpretation of variants in cancer
CM	conditioned medium
CR	complete response
CRIZ	crizotinib
EGFR	epidermal growth factor receptor
ENSAR	ensartinib
ENTRE	entrectinib
EMA	European Medicines Agency
EML4	echinoderm microtubule-like -associated protein 4
EMT	epithelial mesenchymal transition
FAK	focal adhesion kinase
FDA	Food and Drug Administration of the United States of America
IGF-1R	insulin-like growth factor-1 receptor
IL-3	interleukin 3
LC	lung cancer
LOR	lorlatinib
NSCLC	non-small cell lung cancer
MD	molecular docking
ORR	objected response rate
OS	overall survival
pALK	phospho-ALK
PD	progressive disease
PDB	protein data bank file
PFS	progression-free survival
PR	partial response
RMSD	root means square deviation
ROC	receiver operating characteristic
RTK	receptor tyrosine kinase
SCLC	small cell lung cancer
SD	stable disease
SEM	standard error of the mean
tALK	total ALK
TD	trimerisation domain
TKI	ALK tyrosine kinase inhibitor
TRKA/B/C	tropomyosin receptor kinase A/B/C
V1	variant 1
V2	variant 2

LIST OF ABBREVIATIONS

V3a	variant 3a
V3b	variant 3b
WT	wild type

1 Introduction

1.1 General diagnosis and treatment of Non-small cell lung cancer (NSCLC)

Lung cancer (LC), a malignancy originated in the lungs, is a leading cause of cancer death worldwide [1], with an estimated 164,600 deaths in 2021 [2]. Small cell lung cancer (SCLC) and non SCLC (NSCLC) are two major histological classes of LC. NSCLC can be further divided into three histological subtypes: ❶ squamous cell carcinoma (SCC), ❷ adenocarcinoma (AdC), and ❸ large cell carcinoma (LCC) [1].

SCLC is an aggressive neuroendocrine tumor and accounts for approximately 15% of LCs [3]. It arises often in heavy smokers and is characterized by high aggressivity and early metastatic spread [4]. Thus, SCLCs are frequently diagnosed at advanced stage and thus rarely resectable, which hampered the genomic characterization of SCLC. Consequently, chemotherapy remains the first-line treatment [5-7].

Unlike SCLC, NSCLC accounts for the vast majority (85%) of LCs [3] and behaves less aggressive. Non-smokers are mainly afflicted with NSCLC, predominantly AdC [8]. As other malignances, staging is a very important assessment in NSCLC, which guides the determination of how hazardous the cancer is and leads to an optimal treatment strategy. The most often used staging system is that of the International Union against Cancer (UICC, unio internationalis contra cancrum), and four stages (I – IV) with several substages are known in LC based mostly on the TNM (tumor, lymph node and metastasis) classification [9]. For early-stage NSCLC (stage I to IIIA), curative approaches are possible. Patients usually received surgical resection and/or surgery-adjuvant chemotherapy, which is usually a platinum containing doublette – in most cases are cisplatin together with vincristine, gemcitabine, docetaxel, paclitaxel or etoposide [10, 11]. In this setting, overall 5-year survival rates of 60% for patients with localized NSCLC and 33% of patients with regional NSCLC [12] can be achieved. For advanced or metastatic NSCLC (stage IIIB to IV), no curative approach is possible. Thus, these patients who are treated with platinum containing doublettes (see above) only got a 5-year survival rate of 6% [12] due to local or systemic relapses [13, 14]. This unsatisfactory situation changed in 2004 with the introduction of the first targeted therapy [15]. It was found that activating mutations in the epidermal growth factor receptor (EGFR) gene conferred susceptibility to gefitinib (Iressa®), a specific inhibitor of the tyrosine receptor kinase EGFR, in advanced NSCLCs in an Iressa Pan-Asia Study (IPASS) [15]. This IPASS-study and following clinical trials proved that in advanced NSCLCs, the 12-month rates of progression-free survival (PFS) was significantly improved in the group of patients with activating EGFR-gene mutations who received gefitinib (24.9%) than among

those who received carboplatin-paclitaxel (6.7%) [16-19]. These findings led to the conception that tumor driving genomic alterations might serve as a target for treatment and/or as a biomarker predicting responses of NSCLCs to cancer therapies. IPASS-study thus heralded the beginning of the era of precision medicine in NSCLC.

1.2 NSCLC is a paradigm of precision medicine

In the late 80s, Bert Vogelstein proposed that cancer is a disease of the genome caused by sequential mutations of oncogenes (gain of function) and tumor suppressor genes (loss of function) [20, 21]. In LC, possible reasons for a genomic assault are reflected in the risk factors for NSCLC, including smoking [22, 23], air pollution and thus exposure to activated carcinogens which impair the capacity of DNA repair [24, 25]. The impaired DNA-repair system can result in a gain of mutations, which are called tumor mutation burden (TMB) [26]. Based on sequencing approaches like the TCGA (The cancer genome atlas), some recurrent mutations were attributed to oncogenic drivers of lung carcinogenesis. According to data from cBioPortal (Pan-lung cancer, TCGA [27]), the most frequent ones are: TP53 (68%), PIK3CA(24%), KRAS(23%), KEAP1(15%), EGFR(14%), FGFR1(11%), STK11(10%), PTEN(9%), BRAF(7%), ROS1(6%), ALK(5%), MET(5%), ERBB2/HER2(4%), FGFR4(4%), FGFR2(3%), CTNNB1(2.7%), NRAS(2.6%), FGFR3(2.4%), IDH1(1.7%), HRAS(1.7%), MAP2K1/MEK1(1.7%), IDH2(1.5%).

With this knowledge in mind, it became reasonable to develop drugs – mostly specific monoclonal antibodies or smart drugs that can pass the cell membrane – which bind to the mutated driver or inactivate a pathway. This setting is now known as precision medicine, as the response of a tumor can be predicted on the basis of tumor drivers are activated (oncogenes) or inactivated (tumor suppressor genes) by mutations. These tumor drivers are collectively called biomarkers, and the detection of mutations in biomarkers is known as companion diagnostic as the result would affect the selection of drugs. Such drugs are highly specific for certain structures, in most cases are the biomarker itself, and vary from case to case, so the application of these drugs is known as targeted therapy or personalized medicine. For NSCLC, the first biomarker-drug pair was developed for activating mutations in the EGFR and gefitinib (Iressa®) as mentioned before [15]. Over the years, additional targeted drugs were developed for a variety of biomarkers, especially in NSCLC, so that this tumor entity can be seen as a paradigm for precision medicine today (Table 1). The usefulness of molecular targeted therapies directed against kinases, mainly receptor tyrosine kinases (RTKs) or serine-threonine kinases (STK), was demonstrated in an exploratory study [28]. It included 1,007 patients with advanced NSCLC harboured actionable/targetable mutations, and the patients who received targeted therapy lived significantly longer than those who did not receive targeted therapy (median survival of 3.5 and 2.4 years, respectively). The same was true for patients whose NSCLCs did not harbor actionable driver

mutations (median survival of 2.1 years) [28].

With the increasing of targeted drugs and thus to a certain extend also biomarkers, a variety of genetic alterations had to be detected in different genes in parallel, namely: deletions (del), insertions (ins), complex deletions and insertions (indel), point mutations (SNV, single nucleotide variants), CNV (copy number variations), gene translocations and splice-site mutations, which resulting in exon skipping and are frequently measured as gene-fusion events on the level of RNA. For detection of this multiplicity of different genetic alterations, next generation sequencing (NGS) approaches are used nowadays [29-31]. As NGS, especially the analysis of data, is quite a complex technology, it turns out that analyses should be carried out in specialized centers, which leads to nNGM (national Network Genomic Medicine, lung cancer) in Germany. In this network, diagnostic centers diagnose 26 biomarker genes that are biomarkers for ❶ an EMA (European Medicines Agency) approved therapy, ❷ inclusion of patients into clinical trials (Table 1). These biomarkers include: *ALK* (RTK) [32], *ROS1* (RTK) [33], *BRAF* (STK) [34, 35], *KRAS* (GTPase) [28, 36], *RET* (RTK) [37], *MET* (RTK) [38, 39], *NTRK1*, *NTRK2*, *NTRK3* [40, 41], and *HER2* (RTK) [42]. ❸ Additionally, modifier genes *STK11* [43, 44] or *KEAP1* [45] were included, as well as genes supporting other clinical decisions such as TP53 [46] allowing discrimination of multiple primary tumors from metastases. Taken together, as a critical prerequisite for personalizing targeted therapy, the molecular pathological detection of driver mutations has become an integral part in the routine diagnostic procedure for patients with NSCLC.

Table 1 The *nationale Netzwerk Genomische Medizin* (nNGM) diagnostic panel for NSCLC (genetic level). The detection of expression, like PD-L1 are not mentioned here. Companion *biomarkers* with EMA approved drugs are given in italics.

nNGM-Panel (NSCLC)	
DNA-level	RNA-level
<i>ALK</i>	<i>ALK</i>
<i>BRAF</i>	<i>MET</i>
CTNNB1	<i>NTRK1, NTRK2, NTRK3</i>
<i>EGFR</i>	<i>RET</i>
ERBB2 (HER2)	<i>ROS1</i>
FGFR1, FGFR2, FGFR3, FGFR4	
IDH1, IDH2	
KEAP1	
<i>KRAS, NRAS, HRAS1</i>	
MAP2K1 (MEK1)	
<i>MET</i> (inkl. Exon14 skipping)	
PIK3CA	
PTEN	

ROS1

STK11

TP53

1.3 ALK rearrangements in NSCLC

1.3.1 ALK biology and oncogenesis

Among these targetable oncogenes, ALK (anaplastic lymphoma kinase) is a very special target for several reasons: ❶ activation of ALK in NSCLC usually results from translocations that lead to gene fusions, which place the kinase domain of ALK (exon 20) under the control of an active promoter/enhancer, promoting abnormal and unregulatable overexpression of ALK that drives neoplastic growth. ❷ Relapse of patients with NSCLC induced by ALK translocation after treatment with ALK inhibitors is mostly due to ALK mutations in the kinase domain encoded by exon 20, i.e. on-target mutations, rather than due to bypass pathways activation. ❸ There are in the moment 5 EMA-approved targeted ALK specific inhibitors: Crizotinib, Ceritinib, Alectinib, Brigatinib, Lorlatinib that can be used as the first or subsequent lines therapy (for details see: 1.4 and 1.5).

ALK rearrangements are the predominant fusion mutations occurring in approximately 5-6% of NSCLCs [47], and are commonly found in non- or light-smokers at younger age [48, 49] in contrast to KRAS mutations, which are strongly associated with smoking [50]. Studies showed a significant higher rate of ALK rearrangements in patients with advanced NSCLC (11.3%) compared to those in early-stage NSCLCs (4.3%), indicating that it is a later event in the carcinogenesis process. This also underlines the importance of ALK-gene fusions as a key driver, as it is associated with the occurrence of malignant transformation of lung epithelial cells and therefore detected in advanced disease [51]. NSCLCs harboring rearranged ALK-genes/fusion proteins are also called ALK-positive NSCLCs for simplicity.

Under physiological conditions, ALK proteins locate on cell membranes and are only highly expressed in the nervous system or primordial anlagen of lungs during embryogenesis. The ALK-gene encodes an RTK belonging to the insulin receptor superfamily and is thus the starting point of a signaling pathway. Like other RTKs, ALK proteins consist of three structural domains: the extracellular ligand-binding domain, the transmembrane region and the intracellular tyrosine kinase (TK) domain [52] (Figure 1). Native ALK signaling is activated by extracellular ligand-mediated ALK dimerization and subsequent autophosphorylation and activation of intracellular tyrosine kinase domains [53, 54]. Little is known about ALK activation under physiological conditions, only Augmentor α (AUG α) and Augmentor β (AUG β) have been recognized as ALK ligands [55]. When ALK translocates on a genomic level resulting in a fusion transcript and protein, the fusion partner determines the subcellular localization. Moreover, the activation of ALK becomes independent of ligand-binding simply

due to the overexpression of ALK proteins and the provision of a dimerization domain expressed by the fusion-partner [56] (Figure 1). In the end the activation of ALK in the natural context or as a mutant fusion-protein results in the downstream activation of several signaling pathways, including the RAS/RAF/MAPK/ERK1/2-, the JAK/STAT- and the PI3K/AKT-pathway, and are thus involved in cell proliferation and mediate cell survival [57, 58] [59]. [60].

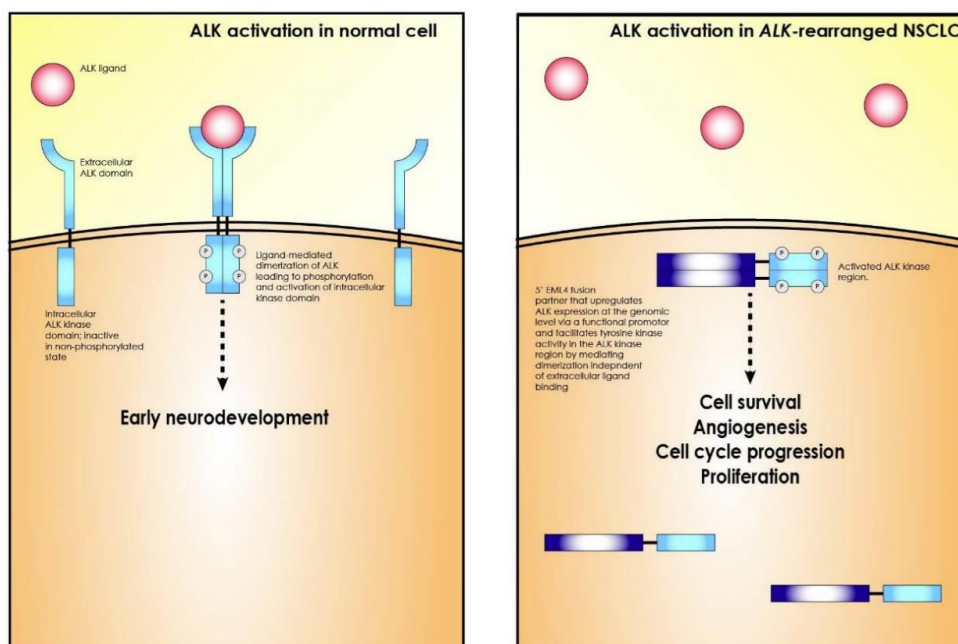


Figure 1 Biology and oncogenesis of the ALK oncogene. Left, ALK activation in normal cells; right, ALK activation in *ALK*-rearranged NSCLC. Graph from *Le T, 2017, ALK alterations and inhibition in lung cancer. Seminars in Cancer Biology, Volume 42, Pages 81-88* [61].

1.3.2 *EML4-ALK* fusion gene

EML4-ALK fusion genes (echinoderm microtubule-associated protein-like 4) were the first identified and the most commonly found ALK rearrangements reported in NSCLC by far (3%-5%) [32, 62].

The *EML4* gene encodes echinoderm microtubule-associated protein-like 4, which is known to be involved in the biology of microtubules: ❶ formation and stability of microtubules [63, 64], ❷ organization of the mitotic spindle and proper attachment of kinetochores to microtubules [65], and ❸ progression of mitosis by recruiting NUDC (nuclear migration protein nudC) to the mitotic spindle [65]. *EML4* is highly expressed in normal epithelial cells of the lungs (Expression Atlas; <https://www.ebi.ac.uk>). On the molecular level, *EML4* is organized into ❶ a trimerisation domain (TD), ❷ basic region, ❸ hydrophobic motif (HELP), and ❹ Trp-Asp repeats domain (WD repeat), which is also called TAPE domain (Figure 2). *EML4* and *ALK* genes are both located on the short arm of chromosome 2 (Chr 2: *EML4*: 42.17 – 42.33 Mb, *ALK*: 29.19 – 29.92 Mb) but are transcribed in opposite directions. Thus, gene-fusion events are the result of inversions leading to *EML4-ALK* fusion genes [32]. Due

to different breakpoints of *EML4*, multiple isoforms of the *EML4*-*ALK* fusion gene are formed (Figure 2). Today, at least eleven *EML4*-*ALK* variants have been identified [32, 62, 66, 67]. The most common variants are ❶ variant 1 (V1, *EML4* exon13 to *ALK* exon20, E(13)A(20)), ❷ variant 2 (V2, *EML4* exon20 to *ALK* exon20, E(20)A(20)), and ❸ variant 3a/b (V3a/b, *EML4* exon6a/b to *ALK* exon20, E(6a)A(20), E(6b)A(20)) [68-71]. Since all isoforms include the *ALK* intracellular tyrosine kinase domain, which located in the region encoding exon20, and the TD domain of *EML4* gene (Figure 2, Table 2), *ALK* activation in *EML4*-*ALK* is suggested to be primarily driven by the TD domain of *EML4*, which drives autophosphorylation following self-association of the kinase domains due to a possible trimerization and thus autoactivation independent of ligand binding [72].

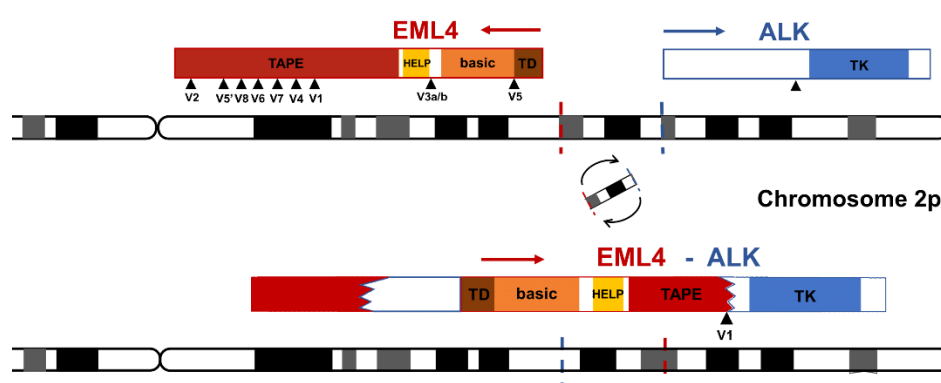


Figure 2 Protein domain structures of *EML4* and *ALK* and chromosomal rearrangement for *EML4*-*ALK* variants. Genomic organization and protein domain structures of *EML4* and *ALK* (**upper** panel) and chromosomal rearrangement for *EML4*-*ALK* variant 1(V1) (**lower** panel). **Red**, *EML4* protein domain structures and functional motifs; **blue**, *ALK* protein domain structures and functional kinase domain; **arrowheads**, breakpoints in *EML4* and *ALK*. TD, trimerisation domain; HELP, hydrophobic motif; TAPE, tandem atypical β -propeller; TK, tyrosine kinase.

Table 2 *EML4*-*ALK* variants and their properties.

Variants	Gene fusion points	Frequency	Structure features in <i>EML4</i>			
			incomplete TAPE	HELP	basic	TD
V1[32, 73, 74]	E13;A20	40-50%	✓	✓	✓	✓
V2[32, 74]	E20;A20	10%	✓	✓	✓	✓
V3a/b*[74]	E6a/b;A20	30-35%	⊗	⊗	✓	✓
V4[74]	E15del60;del71A20	<1%	✓	✓	✓	✓
V5[75]	E2;A20	<1%	⊗	⊗	⊗	✓
V5'[76]	E18;A20	<1%	✓	✓	✓	✓
V6[77]	E13;ins69A20	<1%	✓	✓	✓	✓
V7[77]	E14;del12A20	<1%	✓	✓	✓	✓
V8a[67]	E17;ins30A20	<1%	✓	✓	✓	✓
V8b[67]	E17ins61;ins34A20	<1%	✓	✓	✓	✓

*V3b contains an extra 11 amino acid (33bp) insertion in exon 6 compared with V3a

1.4 Targeting *EML4-ALK* fusion genes

Due to the ligand-independent activation of ALK in lung epithelial cells, these cells became neoplastically transformed by their fused ALK-genes, but conversely, the growth and survival of these cells rely on the activity of the ALK-fusion protein. This property has been termed as oncogenic addiction. Consequently, when specifically targeting ALK using tyrosine kinase inhibitors (TKIs), a rapid and significant reduction in expansion and survival of tumor cells had been observed in ALK-positive patients [71, 78-81]. Like other kinase inhibitors, TKIs are generally by nature designed as ATP analogs, which are ultimately resulting in the blockade of kinase activation by competing with ATP for the binding sites (ATP-binding pockets) [82, 83]. Alternatively, some TKIs also work by inducing conformational alterations in the target kinases resulting in their inactivation [84, 85]. Together, these TKIs are collectively known as ALK tyrosine kinase inhibitors (ALK-TKIs, Table 3).

1.4.1 First-generation TKI– crizotinib

Crizotinib is the founder and the only member of the group of first-generation ALK inhibitors. It was originally designed for targeting the MET (mesenchymal epithelial transition) RTK – also known as hepatocyte growth factor receptor (HGFR) or scatter factor (SCF) - carrying activating mutations. Unexpectedly, in a phase I clinical study which enrolled patients with advanced NSCLC in 2006, cases with rearranged ALK were found to be extremely sensitive to crizotinib. Therefore, the study was modified to an expanded cohort for ALK-positive NSCLCs [86]. The efficacy results for this extended cohort were significant so that a subsequent phase II single-arm clinical trial, PROFILE1005, was launched and demonstrated excellent responses of patients with ALK-positive NSCLC to crizotinib [87]. Due to the significant responses in both phase I and phase II trials with an overall response rate (ORR) of 57% and 54%, respectively, crizotinib received accelerated approval in 2011 by the FDA for the treatment of patients with ALK-positive NSCLC [88]. In the phase III clinical trials PROFILE 1007 and PROFILE 1014, the efficacy of crizotinib compared to that of standard chemotherapy in patients who had failed at least one prior platinum-containing regimen and in patients who had not received previous treatment, was compared respectively [79, 80]. Both studies indicated that crizotinib was superior to the standard first-line (at that time) of pemetrexed plus platinum chemotherapy, and the ORR were 65% with crizotinib and 20% with chemotherapy [79]. As a result, in October 2012, crizotinib was also approved by EMA for the treatment of ALK-positive NSCLC patients, irrespective of whether they received prior platinum-containing regimen or not.

Unfortunately, despite the satisfactory initial response of crizotinib, most patients develop resistance and subsequently relapsed within a year [89]. The main cause are acquired resistance-mediating mutations in the kinase domain of the ALK gene.

1.4.2 Second-generation TKIs- ceritinib, alectinib and brigatinib

After crizotinib-resistance mutations were identified, structurally different and more potent inhibitors were developed. They are collectively known as second-generation TKIs. The approval of second-generation ALK inhibitors followed a similar path as that of crizotinib from preclinical studies to approval.

Ceritinib

Ceritinib was the first second-generation (first in class) ALK inhibitor tested in clinical trials. First, a phase I clinical trial (ASCEND-1) showed a durable systemic response and intracranial efficacy of ceritinib in patients with ALK-positive NSCLC (ORR of 56%), regardless of brain metastasis status and prior treatment with an ALK inhibitor or not [90]. Subsequently, the phase II trial (ASCEND-2) further evaluated the response to ceritinib in patients with ALK rearranged NSCLC who had received two or more prior treatment regimens (chemotherapy, one or more platinum-based regimen) [91]. It showed a consistent activity of ceritinib as it behaved in ASCEND-1, with an ORR of 45% [91]. Accordingly, ceritinib was originally conditionally approved by the EMA in 2015 for the treatment of ALK-positive patients who progressed or were intolerant to crizotinib, and was completely approved in 2017. Notably, although there were no head-to-head trials comparing ceritinib and crizotinib, various meta-analyses of cross-clinical trials had been conducted and suggested that ceritinib was associated with prolonged progression-free survival (PFS) (hazard ratio [HR] of 0.50), OS (HR of 0.62) and better ORR (HR of 1.57), compared with crizotinib [92].

Alectinib

Alectinib is a potent and highly selective inhibitor of ALK tyrosine kinase [93, 94]. The process from phase I clinical trials to first-line approval for alectinib was particularly fast, reflected in that after the good tolerability and high activity of alectinib in patients with ALK rearranged NSCLC was proved in phase I/II clinical trials [95, 96], alectinib rapidly progressed to a head-to-head comparison with the standard first-line drug crizotinib in phase III studies. And in the phase III ALEX trial [97], alectinib was shown to be significantly superior to crizotinib, with a median progression-free survival (mPFS) more than three times longer than crizotinib. Therefore, in 2017, alectinib was approved by the EMA for patients with ALK-positive NSCLC and patients who progressed after crizotinib.

Brigatinib

Brigatinib is a TKI displaying a broader *in vitro* activity against various kinases, including ALK, insulin-like growth factor-1 receptor (IGF-1R) and ROS1 besides others [98, 99]. In the phase II ALTA trial, brigatinib demonstrated a robust PFS of 12.9 months with high ORR (54%) in crizotinib-resistant patients [100, 101]. Subsequently, the phase III ALTA-1L trial performed

a head-to-head study of brigatinib and crizotinib. Here, brigatinib was shown to have a better efficacy and tolerability compared to crizotinib, with PFS of 29.4 months vs 9.2 months [102]. Thus, brigatinib was approved by the EMA in November 2018 in treating ALK-positive NSCLC patients, regardless of their prior treatment of ALK-TKIs.

1.4.3 Third-generation TKI —lorlatinib

Since still not all mutations found in crizotinib are effectively targeted by second-generation ALK TKIs, and resistance mutations have emerged in the context of using second-generation TKIs. Thus, starting from the chemical structure of crizotinib, derivatives were specifically designed to target such mutations. Lorlatinib is founder and only member of this group of third-generation ALK Inhibitors. In preclinical models, lorlatinib showed a 62-fold higher activity against rearranged ALK compared to crizotinib [103]. Moreover, in early clinical trials, lorlatinib showed an effective and robust systemic and intracranial anti-tumor activity in both primary ALK-positive NSCLC patients and patients who progressed after crizotinib treatment [104, 105]. Based on these results, the FDA accelerated the approval of lorlatinib in 2018. And in 2019, the EMA followed approving lorlatinib for ALK-positive NSCLC patients, especially those who progressed under the treatment of other ALK-TKIs. Subsequently, the therapeutic efficacy of lorlatinib in tumors carrying ALK-resistant mutations was evaluated [106]. In this study, lorlatinib was exerted greater efficacy in tumors with ALK mutations compared to those without ALK mutations (ORR of 69% and 27%).

1.4.4 Others

Entrectinib

Entrectinib was developed as a potent inhibitor of the RTK tropomyosin receptor kinase A/B/C (TRKA/B/C, genes: NTRK1, -2, and -3) but also ROS1 and ALK. It was evaluated in two phase I studies (Alka-372-001 and STARTRK-1 [84]) in patients with advanced or metastatic solid tumors with rearrangements of the TRK-, ROS1- or ALK genes. In total, 26 cases with ALK-rearranged solid tumors were enrolled, among them 19 patients, who received prior treatment with one or more ALK-TKIs, did not respond to entrectinib. The remaining 7 patients who were initially treated with entrectinib had an ORR of 57% (95% CI 25-84%) [84, 107]. Consequently, in 2021, entrectinib was approved only for patients with solid tumours with NTRK-fusion gene and NSCLC patients with ROS1 fusion-genes.

Ensartinib (X-396)

Ensartinib (X-396) is structurally a novel, amino-pyridazine-based small molecule that potently inhibits ALK. It was indicated 10-fold more potent than crizotinib *in vitro* at inhibiting the growth of ALK-positive lung cancer cell lines [108]. After demonstrating that ensartinib is active and generally well tolerated in ALK-positive NSCLC patients [109], a single-arm phase II multicenter trial further confirmed the activity of ensartinib in patients with crizotinib-

refractory ALK-positive NSCLC [110]. Currently, the randomized Phase III multicenter eXalt3 trial is ongoing [111].

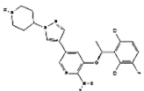
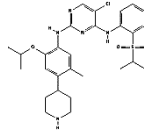
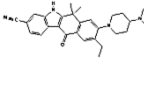
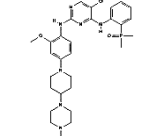
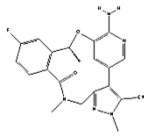
Belizatinib (TSR-011)

Belizatinib is a dual ALK and TRK inhibitor. It showed a robust activity against ALK TKI-resistant tumors in preclinical studies [112]. In a phase I open-label, dose-escalation trial, belizatinib demonstrated a favourable safety profile for ALK-positive NSCLC patients, but further development was halted due to its limited clinical activity [113].

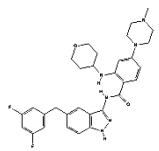
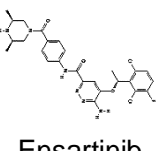
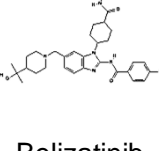
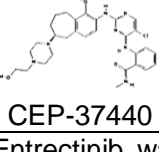
CEP-37440

CEP-37440, a selective inhibitor of focal adhesion kinase (FAK) and ALK, is a novel anti-cancer therapeutic agent under development that has shown potent *in vitro* anti-tumor activity in preclinical studies [114].

Table 3 EMA-approved and unapproved ALK inhibitors used in this study.

ALK-TKI	Generation	Targeted Kinases	Clinical Evidence	EMA approval
 Crizotinib	1.	ALK c-MET ROS1	Phase I/II/III (Complete) [79, 80, 86, 87]	2012.10, first line
 Ceritinib	2.	ALK IGF-1R InsR STK22D	Phase I/II (Complete) Phase III (NCT02393625) Phase IV (NCT02584933) [81, 90, 115, 116]	2015.05 (conditional approval) 2017.07 (complete approval); first line
 Alectinib	2.	ALK	Phase I/II (Complete) Phase III (NCT03596866) [78, 96, 117-119]	2017.02; first line
 Brigatinib	2.	ALK	Phase I/II (Complete) Phase III (NCT02094573, NCT03596866) [99, 120-122]	2018.11; first line
 Lorlatinib	3.	ALK ROS1	Phase I (Complete) Phase II (NCT01970865) Phase III (NCT03052608) [119, 120, 123]	2019.05; second line

INTRODUCTION

 Entrectinib	Approved but not for ALK	TRKA/B/C ROS1 ALK	Phase I (NCT02097810) Phase II (NCT03178552, NCT04302025) [84, 120, 124]	2020.07*
 Ensartinib	Unapproved	ALK MET	Phase I (Complete) Phase II (NCT04415320, NCT03737994) [108, 120]	
 Belizatinib	Unapproved	ALK TRKA/B/C	Phase I/IIa (NCT02048488) [113]	
 CEP-37440	Unapproved	FAK ALK	Phase I (NCT01922752) [125]	

* Entrectinib was approved for patients with solid tumours with *NTRK* fusion gene and NSCLC patients with *ROS1* fusion gene

1.5 ALK-TKI resistance mechanisms

Currently, the biggest problem in targeting therapies of cancer is the development of resistances (acquired or secondary resistances) against the targeted drug, which also happens in the treatment of ALK positive NSCLCs using ALK-TKIs. There are two main categories of ALK-TKI resistance mechanisms: ❶ ALK-independent resistance, including the activation of bypass signaling, phenotypic changes in tumor cells, or the type of fusion variants, ❷ ALK-dependent resistance, including ALK resistance mutations.

1.5.1 ALK-independent resistance

Bypass signaling activation and phenotypic changes

One of the ALK-independent resistance mechanisms is the activation of bypass signaling pathways, which enable tumor cells to survive independently of ALK activation. These activated bypass signaling pathways include HER family, including EGFR [126, 127], ERBB3 (HER3) and ERBB4 (HER4) [128], MET [129], IGF-1R [73] and SRC [130].

Epithelial mesenchymal transition (EMT) and small cell lung cancer (SCLC) transformation also contribute to the resistance to ALK-TKIs. This has been reported in ALK-TKI-resistant cell lines and tumor samples [78, 131, 132].

EML4-ALK fusion variants

Another interesting phenomenon of resistance for ALK specific TKIs was found in the context of EML4-ALK fusion variants. As they all contain the same intracellular tyrosine kinase structural domain of ALK but differ at the point of fusion with EML4, the differences in their responses to a certain ALK-TKI can be considered to be ALK-independent. Thus, an additional layer of complexity, lying on the side of the fusion-proteins, is included in the consideration of ALK specific TKIs.

These differences of EML4-ALK variants in distinct biological and molecular properties were first reported by Heuckman et al. [133]. The authors suggested V2, the longest but also most unstable variant, to be more sensitive to ALK-TKIs compared to other variants. There are also several retrospective studies concerning EML4-ALK variants, but no consistent conclusion was demonstrated. NSCLC-patients with V1, V2 and other variants were reported to have longer PFS compared to patients of V3a/b [68]. And V3 conferred accelerated metastatic spread and early treatment failure in ALK positive NSCLC-patients and was thus considered to be a high-risk variant [134]. Conversely, certain studies did not identify differences in the responses to ALK inhibitors based on EML4-ALK variants [135-137]. Therefore, differences in the sensitivity of EML4-ALK variants for ALK-TKIs are required to be addressed.

1.5.2 ALK-dependent resistance

Expectedly, ALK resistance mutations frequently develop under the treatment of ALK-TKIs. In the majority of cases, resistance develops by mutations that change the conformation of the catalytic cleft of the TK domain or reduce binding affinity of inhibitors. Such mutations are frequently found in the tyrosine kinase domain of ALK [84, 85].

Most common mutations in ALK

In detail, the ALK TK domain consists of a small amino-terminal lobe (N-lobe), which consists of a five-stranded antiparallel β -sheet [138], an α C-helix and a conserved glycine-rich loop (P-loop) for ATP-phosphate-binding loop, and a large carboxyl-terminal lobe (C-lobe) (Figure 3). The α C-helix plays an important role in the regulation of active and inactive conformations of ALK, and the most common resistance mutations found in α C-helix were C1156Y [139, 140], F1174C/L/V and I1171T/N/S [78, 141]. The region connecting N-lobe to C-lobe is the hinge region, which interacts with most small molecule inhibitors of protein kinases by forming hydrogen bonds [142]. Here, the super resistance mutation G1202R that contributes resistance to all first- and second-generation ALK-TKIs occurs in C-terminus of hinge residues [78, 140, 143]. The frequent G1269A mutation (4%) is located in the ATP binding pocket and prevents crizotinib binding [78, 134]. In addition, several functionally important residues in ALK: a regulatory R-spine that consists of five discontinuous hydrophobic residues (Cys1182, Ile1171, Phe1271, His1247 and Asp1311) and a catalytic C-spine that

constitute of eight hydrophobic residues (Val1130, Ala1148, Leu1256, Cys1255, Leu1257, Leu1204, Leu1318 and Ile1322) were identified as additional resistance mutations [138, 144] (Figure 3). Since the regulatory spine is important in defining active and inactive states of ALK and the catalytic spine regulates catalysis by directing the binding of ATP [138], the I1171T/N/S and L1256R mutations in these residues thus contribute to ALK-TKI resistance. Moreover, the first reported and most common ALK resistance mutation (7%), L1196M [70, 78], was found at the gatekeeper residue locates near the interaction top of the R-spine and C-spine. Since the gatekeeper residue contributes to the stabilization of the R-spine and define the affinity or binding mode of inhibitors, mutations in gatekeeper residue can thereby interfere TKI binding and seriously affect the activity of inhibitors in ALK [145] (Figure 3).

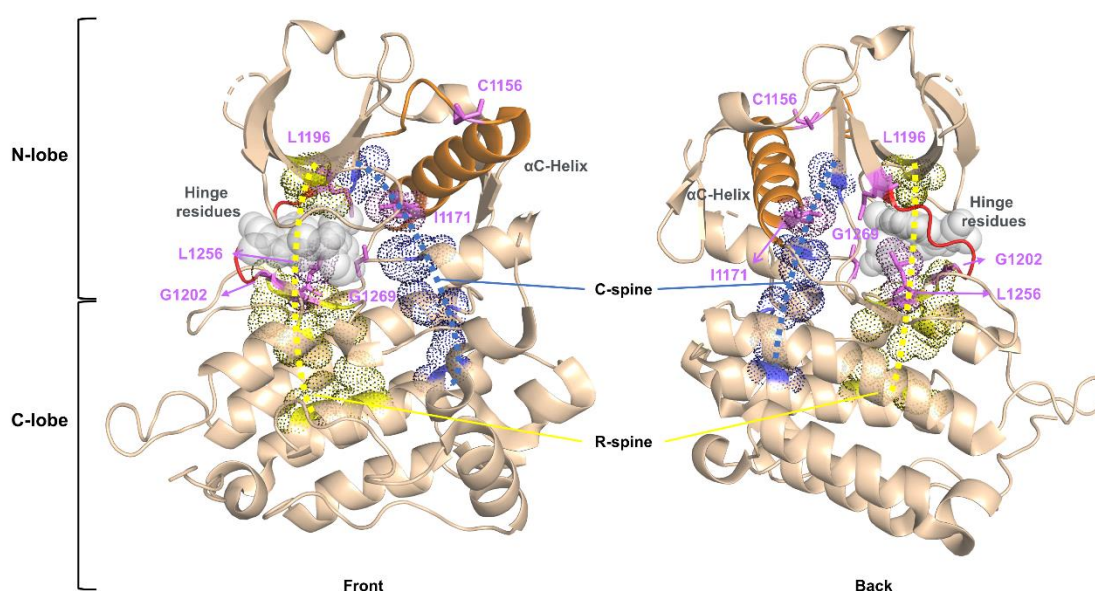


Figure 3 Structure of human wild type (WT) ALK kinase domain depicting domains and commonly found resistance mutations for ALK specific TKIs. The regulatory α C-helix colors in **orange** and the hinge residues colors in **red**. The R-spine is indicated by **yellow dots and yellow dash lines**; C-spine is indicated by **blue dots and blue dash lines**. **Violet text** marks resistance mutations investigated in the work presented here. **Gray spheres** represent lorlatinib thereby indicating the ATP-binding pocket. The structure is visualized based on a protein data bank (PDB) file (PDB ID: 6cdt).

Efficacy of ALK-TKIs varies across ALK resistance mutations

The efficacy of ALK-TKIs varies across ALK resistance mutations, given the structural differences among them. Secondary ALK mutations were observed in 20-30% of patients progressing on crizotinib treatment compared to 56% on second-generation ALK-TKIs [146]. L1196M and G1269A were the most common resistance mutations detected in biopsies from crizotinib resistant tumor samples. Interestingly, G1202R was found in only 2% of post-crizotinib samples but was the predominant resistance mutation in post-second generation ALK-TKIs samples (21-43%) [78]. In general, second- or third-generation ALK-TKIs can overcome resistance to crizotinib, due to their higher affinity for the ALK kinase domain compared to crizotinib. For example, ceritinib shows efficacy against crizotinib-resistant

tumors carrying mutations such as L1196M, G1269A, I1171T and S1206Y [139, 147]. Alectinib showed high efficacy against crizotinib-resistant mutations as L1196M, T1151M/R, C1156Y and F174L/C/V, but not against G1202R [148]. The third-generation ALK-TKI lorlatinib, which was specifically designed for targeting mutations that cause resistance to crizotinib and second-generation TKIs, showed the strongest inhibitory potency against all types of mutations, including the G1202R mutation [106]. However, the same mechanism can also act vice versa as the lorlatinib resistance mutation L1198F enhanced binding of crizotinib to the ALK kinase paradoxically, and therefore sensitized tumor cells to crizotinib again [149]. Such cases highlight the complexity of the emerging ALK resistance mutations, and the importance of taking serial biopsies in the practice to determine the ALK mutation status in recurrent disease. Moreover, it also emphasizes the importance of defining the efficacy of each ALK-TKI against single or combinations of resistance mutations (mutation profile) found in NSCLC patients in order to provide each individual patient with the most efficient and durable targeting strategy in the disease course, and thereby underlines the concept and principle of personalized medicine.

In conclusion, the greatest challenge for the treatment of ALK-positive NSCLC patients, particularly those with ALK-TKIs-resistant mutations, is how to optimally treat these patients with proper ALK-TKIs according to the tumor's ALK mutation status. Thus, the knowledge gained about resistance mutations will ultimately provide benefits for designing the most optimal lines of therapy. Furthermore, since both ❶ the type of mutation and ❷ the variants, in case of EML4-ALK fusions, affecting ALK-TKIs sensitivity, a combined consideration seems to be crucial for selecting the most optimal treatment for individual patients. Unfortunately, there is no study testing the combination of resistance mutations with EML4-ALK variants up to now [150]. This endeavor is undertaken in the present study. Based on clinically reported variant-mutation combinations, this study generated a reliable cellular model (Ba/F3-cells) for drug screening and delineated optimal inhibitor for different mutation-variant combinations. Notably, belizatinib was found to have a very high activity against L1196M mutations in the ALK kinase domain in terms of targeting and molecular dynamics simulations.

2 Materials and methods

2.1 Materials

Chemicals and reagents

Name	Cat. No.	Supplier
Cell culture		
Dimethyl Sulfoxide (DMSO)	D2650-100ML	Sigma-Aldrich
Blasticidin	ant-bl-05	InvivoGen
RPMI 1640	P04-18525	PAN-Biotech
DPBS	P04-36500	PAN-Biotech
Fetal Calf Serum (FCS)	S0165-0910G	Biochrom GmbH
Trypsin/EDTA	L2143	PAN-Biotech
Penicillin-Streptomycin	P06-07050	PAN-Biotech
Opti-MEM™ I Reduced Serum Medium	11058-021	Thermo Fisher Scientific
IL3 Recombinant Mouse Protein	PMC0034	Gibco
Cloning		
LB Broth	L3022-1KG	Sigma-Aldrich
Fast-media Amp Agar	fas-am-s	InvivoGen
Maxima HS Taq DNA Polymerase	EP0601	Thermo Scientific
dNTP	18427088	Invitrogen
Stellar™ Competent Cells	636766	TaKaRa
Ampicillin	A5354	Sigma-Aldrich
GeneRuler 1 kb DNA Ladder	SM0311	Thermo Scientific
Biozym LE Agarose	840001	Biozym
TriTrack DNA Loading Dye (6X)	R1161	Thermo Scientific
Western Blot		
RIPA Buffer (10×)	9806S	CST
PhosSTOP EASYpack	04906837001	Carl Roth GmbH
cOmplete Tablets EASYpack	04693116001	Carl Roth GmbH
SuperSignal™ West Femto Maximum Sensitivity Substrate	34095	Thermo Scientific
Immobilon Western Chemilumineszentes HRP-Substrat	WBKLS0500	Millipore
Milk Powder	T145.3	Carl Roth GmbH

Bovine Serum Albumine (BSA)	A1933	Sigma-Aldrich
PageRuler™ Plus Prestained Protein Ladder	26620	Thermo Fisher Scientific
Protein Assay Dye Reagent Concentrate	5000006	Bio-Rad
Sodium Chloride (NaCl)	7647-14-5	Carl Roth GmbH
Sodium Dodecyl Sulfate SDS	P029.3	Sigma-Aldrich
Sodium Hydroxide (NaOH)	4360.2	Carl Roth GmbH
Tris Base	5429.2	Carl Roth GmbH
Tween-20	A49740100	AppliChem GmbH
Acrylamid/Bis-acrylamid	A3574	Sigma-Aldrich
Ammonium Persulfate	17874	Thermo Scientific
Cell viability		
alamarBlue	BUF012A	Bio-Rad

Consumables

Name	Cat. No.	Supplier
Cell Culture Flasks T25, T75	430639, 430641	Corning
6,12,24 Well Plates	3506, 3512, 3527	Corning
96 Well Plates, flat bottom	Z707902	TPP
35mm Culture Dish	CLS430165	Corning
1.5ml, 2ml SafeSeal Micro Tubes	72706400	Sarstedt
Centrifuge Tubes 15 ml, 50 ml	191015, 191050	TPP
14ml Polypropylene Round-Bottom Tube	352059	Falcon
Pipette Filter Tips 1000µl, 100µl, 10µl	VT0270, 751448, VT0290	Biozym, Biosphere plus
Reagent-Reservoir 25ml	40015	Moonlab
Purple Nitrile Xtra Gloves	0388201-4	Kimberly-Clark Kimtech Science
PVDF (poly-vinylidene difluoride) Membrane	1620177	Bio-Rad
Serological Pipets 2ml, 5ml, 10ml, 25ml	4486, 4487, 4488, 4489	Corning
Cassettes 1.0mm, 1.5mm	10604073, 11559156	novex
Electroporation Cuvettes	EC-002	NEPA Gene

Devices

Name	Supplier
Axiovert 25 Inverted Phase Contrast Fluorescent Microscope	Carl Zeiss
Centrifuge 5417R	Eppendorf
Incubator Cell Culture HERAcell 240i	Thermo Fisher Scientific
Laminar Flow Hood MAXISAFE 2020	Thermo Fisher Scientific
NEPA21 Super Electroporator	NEPA Gene
LiCor Odyssey FC	LiCor
Nanodrop 1000 Spectrophotometer	Thermo Fisher Scientific
HTU Soni130	G.Heinemann
Pipetboy	INTEGRA Biosciences GmbH
Handystep's Electronic	Brandtech
Research Plus Multi-channel Pipettes (100µl, 10µl)	Eppendorf
Research Plus Single-channel Pipette (1000µl, 100µl, 10µl, 2.5µl)	Eppendorf
Shaker D05-10L	neoLab
Sub-cell GT	Bio-Rad
FluorChem TC2	Alpha Innotech
XCell II™ Blot Module	Invitrogen
PowerPac Basic	Bio-Rad

Kits

Name	Cat. No.	Supplier
NucleoSpin Plasmid EasyPure	740727.50	Macherey-Nagel
NucleoBond Xtra Maxi	740414.50	Macherey-Nagel
NucleoSpin Gel and PCR Clean-up	740609.50	Macherey-Nagel
QuikChange II XL Site-Directed Mutagenesis Kit	200522	Agilent

Cell lines

Cell line	Organism	Cell type	No.
Ba/F3	Mus musculus	pro B cells	ACC300
WEHI-3B	Mus musculus	myelomonocytic leukemia	ACC26

Antibodies for Western blot

Antibody	Cat.	Dilution	Supplier
ALK (D5F3) XP Rabbit mAb	3633	1:2000	CST
Phospho-ALK (Tyr1282/1283) (D39B2) Rabbit mAb	9687	1:1000	CST
α -Tubulin (11H10) Rabbit mAb	2125	1:5000	CST
Goat anti-Rabbit IgG (H+L) Cross-Adsorbed Secondary Antibody	G-21234	1:15000	Invitrogen

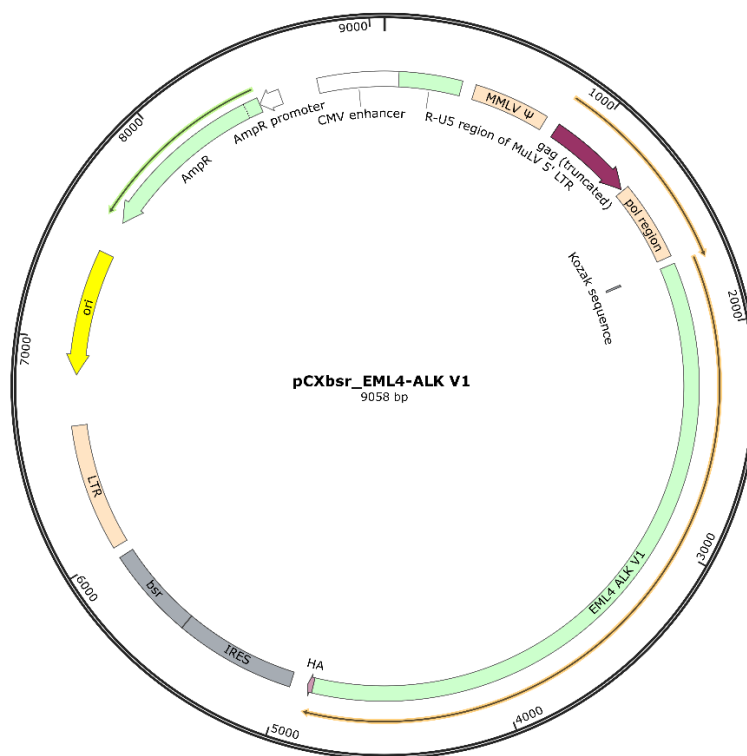
Buffers and components

Buffer	Components
TAE Buffer, 50X	95.05g EDTA Disodium Salt 242g Tris-base 57.1ml 100% Glacial Acid up to 500ml with ddH ₂ O
LB Medium	20g LB Broth up to 1L with ddH ₂ O Sterilize by autoclaving at 121°C for 15 minutes and stored at 4°C
LB Agarose Plates	1 pouch Fast-media Amp Agar up to 200ml with ddH ₂ O Microwave 2 minutes and poured into dishes
APS, 10% (w/v)	5g Ammonium Persulfate up to 50ml with ddH ₂ O
Blocking Buffer, 5%	5g Low Fat Milk Powder 100ml 1x TBS/T (0.1%)
Laemmli Buffer, 4x	10% (w/v) SDS 0.5M Tris-HCl (pH 6.8) 20% (v/v) Glycerol 10% (v/v) β -Mercaptoethanol up to 10ml with ddH ₂ O
Lysis Buffer, 1x	1ml 10x RIPA Buffer 1 piece of Protease Inhibitor cocktail cOmplete™ ULTRA Tablets 1 piece of phosphatase inhibitor PhosSTOP up to 10ml with ddH ₂ O

MATERIALS AND METHODS

Running Buffer, 10x	30g Tris Base 144g Glycerol 10g SDS up to 1000ml with ddH ₂ O
TBS Buffer, 20x	121g Tris Base 80g NaCl up to 1000ml with ddH ₂ O adjusted pH 7.5 with NaOH
Transfer Buffer, 10x	30g Tris Base 144g Glycerol up to 1000ml with H ₂ O
Tris-HCl, 1x pH 6.8	1M Tris Base 100ml ddH ₂ O adjusted pH 6.8 with NaOH
Tris-HCl, 1x pH 8.8	1.5M Tris Base 500ml ddH ₂ O adjusted pH 8.8 with NaOH

Plasmid



Map of pCXbsr vector with EML4-ALK V1 insertion (Visualized by SnapGene 4.3.6).

Primers

Name	Sequence
Mutagenesis	
G1269A Fwd	GAGTGGCCAAGATTGCAGACTTCGGGATGGC
G1269A Rev	GCCATCCCGAAGTCTGCAATCTTGGCCACTC
L1196M Fwd	CCCGGTTTCATCCTGATGGAGCTCATGGCG
L1196M Rev	CGCCATGAGCTCCATCAGGATGAACCGGG
C1156Y Fwd	TGAAGACGCTGCCTGAAGTGTATTCTGAACAGGACGAAC
C1156Y Rev	GTTTCGTCCTGTTCCAGAATACACTTCAGGCAGCGTCTTCA
I1171T Fwd	CATGGAAGCCCTGATCACCAGCAAATTCAACCACC
I1171T Rev	GGTGGTTGAATTTGCTGGTGATCAGGGCTTCCATG
F1174L Fwd	CCCTGATCATCAGCAAACCTCAACCACCAGAACA
F1174L Rev	TGTTCTGGTGGTTGAGTTTGCTGATGATCAGGG
G1202R Fwd	GCTCATGGCGGGGAGAGACCTCAAGTC
G1202R Rev	GACTTGAGGTCTCTCCCCGCCATGAGC
L1152R Fwd	GGCTGTGAAGACGCGGCCTGAAGTGTGCT
L1152R Rev	AGCACACTTCAGGCCGCGTCTTCACAGCC
Sanger Sequencing	
ALK HA Pacl Rev-	TACCGCGGCCGCTTAATTAAC
EML4-ALK seq Fwd	TGCGCGGTCCGCCAATTAC
EML4-ALK seq Fwd	GTGCAGTGTTTAGCATTCTTGGGG
EML4-ALK seq Fwd	GCTGCCAGTTAAGTGGATGCC
EML4-ALK seq Fwd	CCCTCTTCGCTGACTGCCA
EML4-ALK seq Fwd	GGAAGGTGCACTGGACATTCCA
EML4-ALK seq Fwd	ACGACCATCACCAGCTGAAAAGTC
EML4-ALK seq Rev	GGGTCCTGGGTGCAGTATTCAAT
EML4-ALK seq Rev	GGGTGATGTTTTTCCGCGGC
EML4-ALK seq Rev	CCCCGGTCGGAAGAAGG
EML4-ALK seq Rev	GCCGCCTTTAGCACAGTGATT
EML4-ALK seq Rev	GCCTTTCCTTCTGCTACAGCTC

2.2 Methods

2.2.1 Information acquisition online

The Clinical Knowledgebase (CKB, <https://ckb.jax.org/> [151]) and clinical interpretation of variants in cancer (CIViC, <https://civicdb.org/> [152]) were used to obtain a combination of information of ALK resistance mutations and fusion variants. Mutations in NSCLC associated

with drug resistance to ALK-TKIs were chosen and corresponding information regarding fusion variants and patients' responses was retrieved through literature searches in Pubmed (<https://pubmed.ncbi.nlm.nih.gov/>). All information was then collated and summarized.

2.2.2 Mutagenesis

Site-directed point mutagenesis was performed using the QuikChange II XL Site-Directed Mutagenesis Kit (Agilent) according to the instruction manual. Mutagenic primers (See 2.1 Materials, Primers, Mutagenesis) containing desired mutations, which were designed with the online primer design program provided by the kit manufacturer (www.agilent.com/store/primerDesignProgram.jsp).

The retroviral vector pCXbsr containing wildtype EML4-ALK in V1, V2, V3a and V3b, which were obtained from MSc. Meng Wang [153], served as the DNA template for site-directed mutagenesis. Thermal cyclings were proceeded according to the standard procedure given in the manual. Reaction products following thermal cycling were checked by electrophoresis on 2% (w/v) agarose gels. If bands were observed on agarose gels, DpnI hydrolysis was added to hydrolyze non-mutated templates and subsequently, mixtures were transformed into XL10-Gold competent E.coli cells. LB agar plates with transformed bacteria were incubated at 37°C in an incubator overnight.

2.2.3 Gel electrophoresis

Gel trays with combs were horizontally fixed in the gel caster in advance. Proper amounts (1.4g for 70ml, 4g for 200ml) of LE Agarose was weighed and added into 1X TAE buffer to reach a final concentration of 2% (w/v). Mixed solutions were then heated in a microwave oven until agarose was uniformly dissolved. After cooling for 2 minutes, GelRED dye was added into the solution at a ratio of 1 µL/20 mL and mixed well. Next, the agarose solution was poured into the fixed gel tray and allowed to cool and solidify at room temperature.

To prepare samples for loading, 5µl plasmid DNA sample or reaction products were mixed with 1µl 6x Trirack loading buffer. The mixture was carefully added to gel trays using a micropipette. After adding the sample, gel electrophoresis was kept running at constant voltage of 110V for 40-60min. When finished, gels were taken out from the tank and placed under the UV-illuminator. Gel bands at expected position were cut out and purified using NucleoSpin Gel and PCR clean-up kit followed by the standard procedure. All pictures were taken by AlphaEasyFC.

2.2.3 Colony PCR and sequencing

After overnight incubation of LB agar plates containing transformed competent cells with mutated plasmids, plates were taken out of the incubator on the next day. Colonies randomly picked from LB agar plates using pipette tips and were transferred into Eppendorf tubes containing each 100µl LB medium and incubated on a shaker at 300 rpm at 37°C for one

hour. For amplifying the expected region (the region spanning the mutagenesis sites), the respective mutagenic forward together with the reverse primer from the pCXbsr vector backbone, which located downstream of the mutagenic site, were used. The components for PCR reactions are listed below:

10X Maxima Hot Start Taq Buffer	5µl
dNTP Mix	5µl
Forward Primer (Mutagenesis Primer)	500nM
Reverse Primer (Vector Primer)	500nM
25mM MgCl ₂	2mM
Bacterial suspension	2µl
Maxima Hot Start Taq DNA Polymerase	1.25U
Nuclease-free Water	to 50µl

All reagents were well mixed and were conducted using recommended thermal cycling conditions:

Step	Temperature, °C	Time	Cycles
Initial denaturation	95	8min	1
Denaturation	95	1	25-30 cycles
Annealing	T _m -5	1	
Extension	72	1min/kb	
Final Extension	72	10	1
Hold	4	10	1

Later, PCR products of the expected size were confirmed by gel electrophoresis on a 2% (w/v) agarose gel (see 2.2.3). And gel bands at the expected position were cut out, purified (see 2.2.4) and sent out for sequencing (Eurofins Supreme Sanger Sequencing). Results were aligned employing plasmid sequences by Snapgene 4.3.6.

2.2.4 Plasmid DNA purification

NucleoSpin plasmid easypure kits were used for purification of small-scale plasmid DNA (mini preps) whereas Nulceobind xtra maxi kits were used for large-scale plasmid DNA, which was required for electroporation (maxi preps). Cells for miniprep were grown in 10ml LB media with 100 µg/mL ampicillin and cells for maxiprep were grown in 200 ml LB media with 100 µg/mL ampicillin for 12-16 hours at 37°C, 180rpm. Then cells were spun down at

5000rpm for 15min and supernant was discarded. Subsequently, cell precipitates were handled according to the user's guides. Finally, plasmid DNA concentration was measured with a Nanodrop 1000 Spectrophotometer.

2.2.5 Cell culture

Thawing Frozen Cells

Frozen cells were taken out of -80°C fridge or liquid nitrogen. Cells were transferred on ice and quickly thawed in 37°C water bath. Later, thawed cells were added into a pre-prepared 15ml falcon tube with 6-7ml fresh medium and then centrifuged at 1200rpm for 4min. The supernant was discarded and the cell precipitates were washed once with PBS. At last, cells were resuspended in 4-5ml medium and seeded into a T25 flask.

Production of interleukin 3 conditioned medium (IL3-CM)

As the growth of parental Ba/F3 cells is dependent on the presence of interleukin 3 (IL-3), WEHI-3B cell line, which spontaneously releases IL-3, was used for production of IL-3-CM. Both cell lines were purchased from DMSZ (<https://www.dsmz.de/>). First, WEHI-3B cells (DSMZ, ACC 26, LOT#10) were used to produce IL3-CM. WEHI-3B cells were thawed and seeded into T75 flask with 20ml of RPMI1640 medium containing 5% (v/v) FBS and 1% (v/v) penicillin/streptomycin (100U/mL penicillin, 0.1µg/mL streptomycin, R10). Cells were detached using Trypsin/EDTA and were expanded into two T75 flask when they reached 50-60% confluence. When the medium turned orange, 50ml fresh R10 was added to each flask. Conditioned medium (CM) was harvested when medium turned yellow and cells began to detach. Therefore all medium in the bottles was collected, centrifuged at 2000rpm for 4min at 4°C, supernatant sterile filtered using sterile syringe filter with a 0.45µm pore, aliquoted into 15ml Falcon tubes and finally stored at -20°C for subsequent use.

Optimization of IL3-CM concentration in Ba/F3 cells

Now, Ba/F3 cells were thawed and resuspended in 5ml R10. Cells were seeded for experiments at 1×10^3 /well into 96 cluster well plates and incubated with increasing amounts of IL3-CM as followed:

IL3 [v/v %]	NC	2.5	5	10	15	20	PC
-------------	----	-----	---	----	----	----	----

NC, R10 medium without IL-3; **PC**, R10 with 10ng/ml recombinant IL3 (Gibco, PMC0034).

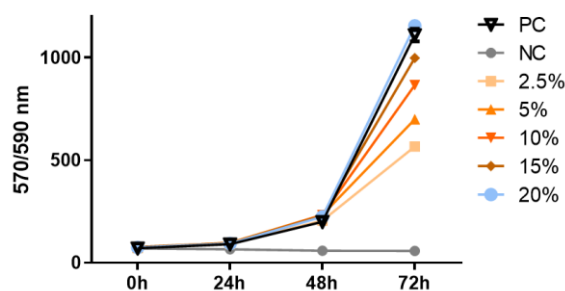


Figure 4 Cell viability of Ba/F3 cells with different concentration of IL3-CM. In the current case, cells with 20% IL3-CM (**blue line**) grew comparably well as cells cultivated in the presence of recombinant IL3 (**black line**). Thus 20% (v/v) addition of CM was the concentration that was chosen for subsequent experiments.

Cell viability was measured daily applying alamarBlue assays for 3-5 days and the concentration which stimulated the best growth of Ba/F3 cells was used in subsequent experiments (Figure 3).

Cryopreservation of cells

To cryopreserve cells, WEHI cells detached by Trypsin/EDTA and resuspended in fresh medium. Ba/F3 were directly collected and centrifuged. Collected cells were centrifuged at 1200rpm for 4min at RT. Supernant was aspirated and cell precipitates were resuspended in freezing medium (90% FCS and 10% DMSO). Cell suspensions were quickly aliquoted into cryogenic vials on ice and transferred into Nalgene freezing container. Subsequently, the freezing container containing the cell vials was stored at -80°C or liquid nitrogen.

2.2.6 Electroporation

The concentration of plasmid DNA got from maxiprep was adjusted to $1\mu\text{g}/\mu\text{l}$. Ba/F3 cells were collected and resuspended in the serum-free Opti-MEM medium (Invitrogen) in a concentration of $1\times 10^8/\text{ml}$. Then $90\mu\text{l}$ (0.9×10^6) cells and $10\mu\text{l}$ ($10\mu\text{g}$) plasmid DNA were added into an electrotransfection cup (EC-002S) and mixed gently. The cup was quickly placed into the cup chamber of NEPA21. Parameters were settled as followed:

	Voltage (V)	Pulse length (msec)	Pulse interval (msec)	Number of pulses	Decay rate (%)
Poring pulse	16	5	20	2	10
Transfer pulse	20	50	50	5	40

Firstly, the resistance value was measured by pressing " Ω ". If the value was between $30-50\Omega$, electroporation could be proceeded by pressing "Start". After electroporation, a provided pipette was used to aspirate the entire suspension in cup and to transfer it into a 6-well plate with 2ml pre-warmed R10 with IL3-CM. The plated with transfected cells should be transferred into the incubator immediately.

2.2.7 IL3/blastocidin selection and cell cloning

IL3/blastocidin selection

In order to obtain cells that stably expressed transfected DNA, the cells underwent a double selection. Due to the character of Ba/F3, i.e. if EML4-ALK was transferred into Ba/F3 cells, they could survive independently of IL-3; if not, the cells would stop growing or even undergo apoptosis, withdrawal of IL-3 became the first selection process. In addition, since the pCXbsr (bsr=blastocidin resistance) vector contained the bsr gene, the cells underwent a secondary selection by blastocidin.

After transfecting by electroporation, Ba/F3 cells were cultured in R10+IL3-CM medium for 3 days. On Day 4, cells were washed twice with PBS and resuspended in fresh R10 medium without IL3-CM. Cells were maintained under non-IL3 selection until cell proliferation resumed and cell growth reaching 60%-70% confluent. Then 10µg/ml blastocidin antibiotic was added for secondary selection. Cell death occurred rapidly in the very first few days, and they were kept under double selection for at least 10 days.

Cell cloning

Bulk cells that survived under double-selection were subjected to single cell cloning. Surviving cells were collected and diluted to a final concentration of 2×10^4 cells/ml in fresh medium with blastocidin. Then a serial dilution of the cells was performed in falcon tubes until 1-3 cells/100µl. One to three cells were seeded into each well of a 96 well plate and incubated for 10-14 days. At last, the wells containing single-clone were picked and cells in the selected wells were seeded into six well plates for further testing.

2.2.8 Western blotting

Protein sample preparation and concentration determination

For protein lysis, cells were washed twice with 2ml PBS and then resuspended in 100-300µl lysis buffer depending on cell amount. After sonification, samples were centrifuged at maxima rpm at 4°C for 15-30min. Then supernant was collected in a new Eppendorf tube and sample concentration was measured using the Bradford assay. 2 µl of cell lysate was added into 98 µl working concentration of Bradford dye. Samples absorption was measured at 595 nm using a Varioskan (Thermo) luminometer and readouts were compared to the reference curve generated in the same experiment using BSA. Finally, 1:4 volume 4X Laemmli buffer was added to each sample.

SDS-Page and Western blot

8% SDS-polyacrylamide gels were prepared in advance as followed:

8% Resolving gel	Volume (ml)	Stacking gel	Volume (ml)
Water	4.64	Water	1.36
1.5M Tris 8.8	2.5	1.5M Tris 6.8	0.25
10% SDS	0.1	10% SDS	0.02
30% Acylamid	2.66	30% Acylamid	0.34
10% APS	0.1	10% APS	0.02
TEMED	0.006	TEMED	0.002
Total	10	Total	2

Samples mixed with 4x Laemmli buffer were incubated at 95°C for 10-15 min and were then subjected to 8% SDS-polyacrylamide gel electrophoresis with 20-30µg/lane. Gel electrophoresis was kept running under the control voltage at 80V for 20-30min for stacking gel and 110V for 90-120 min for resolving gel. After SDS-Page, gels were cut to proper size and placed between a PVDF membrane and two filter/whatman papers according to the manufacturer's instructions [154]. Transfers were performed using XCell II™ blotting module (Invitrogen) at 25V, 100mA for 90-110min. Membranes after transferring were blocked with 5% milk in TBST for 30-60min and washed 3 times with 0.1% TBST. Then the membrane was incubated with the diluted primary antibody (details are described in Materials<Antibodies for Western blot), which was diluted in 0.1% TBST, at 4°C overnight. On the next day, membranes were washed 3 times with 0.1% TBST to remove the primary antibody and then incubated with the secondary antibody, which was diluted in 5% milk in TBST, for 30-60min at room temperature. Blots were developed with enhanced chemiluminescence (ECL) using Licor Odyssey FC System.

2.2.9 Cell viability assay (IC50)

For IC50 assay, cells were adjusted to a concentration of 2×10^4 /ml and 50µl/well (1000 cells/well) was added into 96 well plate at the first day. Serial dilutions of ALK-TKIs (storage concentration 10mM) were prepared in advance as followed:

Concentration (mM)	Dilution fold
0.5	20
0.167	60
0.05	200
0.0167	600
0.005	2000
0.00167	6000

0.0005	20000
0.000167	60000
0.00005	200000
0.0000167	600000

On Day 2, 2µl pre-diluted ALK-TKIs or DMSO control was added to 998µl R10 to achieve the expected working concentration. Then 50µl/well prepared R10+ALK-TKIs working solution was added to the seeded cells. Triplicates were set up for each treatment concentration. Cells treated with ALK-TKIs were incubated for 48 hours at 37°C before the cell viability test. The cell viability assays were performed with alamaBlue reagent (Bio-rad). 10µl alamarBlue solution was added to each well and the cells were incubated for 3-4 hours at 37°C in incubator. Then, absorbance as an indicator for cell viability was measured at 570 nm using a Varioskan (Thermo) luminometer. Readouts were saved as Excel files and transferred into Prism Graphpad (8.4.3) for IC50 analysis.

The cells expressed BCR/Abl as a negative control in cell viability assay were obtained from my colleague [153].

2.2.10 Molecular docking

To perform molecular docking, the crystal structure profiles of ALK-WT chain A (PDB ID: 6cdt) and ALK-L1196M chain A (PDB ID: 2yhv), which contained the tyrosine kinase domain, were obtained from the PDB (<https://www.rcsb.org/>). The 3D structure of belizatinib was obtained from PubChem (<https://pubchem.ncbi.nlm.nih.gov/>). First, the downloaded pdb file was imported into Autodock version 1.5.6 [155, 156] and crystal water was removed. For the protein structure, all hydrogen atoms were added, lower occupied residue structures were removed, and any incomplete side chains were replaced by Autodock. Gasteiger charges were added to each atom and non-polar hydrogen atoms were incorporated into the protein structure. The structure was then selected as macromolecule and saved as pdbqt file. Similar pre-processing was performed on ligands, i.e. all hydrogen atoms and gasteiger charges were added to each atom and then saved as pdbqt files. The previously saved ALK-L1196M protein structure file in pdbqt format was re-opened using the grid operation and was selected as a macromolecule. The ligand was also imported in the same way and was select as ligand. A grid box was created around the ATP binding pocket in ALK. For docking and calculations, the default parameters of autodock vina were used and ten docked conformations were generated for each compound. The docking of each tested compound was analyzed and scored in terms of energy, hydrogen bonding and hydrophobic interaction between the ligand and kinase. Binding affinities were obtained based on the docking scores [155, 157]. The output of the binding patterns and interactions of ligands with ALK-WT/ALK-L1196M at the ATP-binding pocket was exported and visualized by PyMOL 2.5.1 [158].

To perform redocking, the compound structure of belizatinib with ALK-WT (PDB ID: 4fod)

was downloaded from PDB. Belizatinib was fetched from the corresponding compound structure by PyMOL and further chosen as ligand binding to ALK-WT (PDB ID: 6cdt). Steps for redocking were as described above. Later the reproduced conformation with top score was chosen and compared with bound X-ray conformation. To quantify the difference between the reproduced conformation and the X-ray conformation, the root mean square deviation (RMSD) values, a measure of the differences between samples, were calculated by PyMOL.

2.2.11 Data analysis and statistics

ROC curve

Receiver operating characteristic (ROC) analysis was used to illustrate the response-predictive ability of pIC50 values achieved in this study. The pIC50 value was set as test variable and the responses reported in clinical studies was set as state variable (sensitive=1, resistant=0). ROC curve was drawn by IBM SPSS statistic 23. The best cut-off point that maximized the areas under ROC curves [16], corresponding to the maximal (sensitivity+specificity-1) was calculated. The model with an AUC of 0.7 to 0.8 was considered acceptable, 0.8 to 0.9 was considered excellent, and more than 0.9 was considered outstanding.

Statistical data analysis

An IC50 value was defined as the concentration of an ALK-TKI that the cell viability was reduced by half. It was determined by fitting a dose response curve to the data that was means of triplicates in concentration gradient assay. Readouts measured by Varioskan luminometer were imported into Graphpad Prism 8.4.2. The concentration of ALK-TKIs used in cell viability assay was transformed to logarithms. All values were normalized by comparing with the control group and a nonlinear regression was performed using an equation of log(inhibitor) vs. normalized response. IC50 values were achieved after calculation. Considering dose-dependent inhibition was a logarithmic phenomenon, pIC50, the negative log of the IC50 value in molar, was the logarithmic scale of IC50 and had the nature of normal distribution. It provided an easier way to calculate the arithmetic mean value and standard deviation, while IC50 could not. Thus, all IC50 data were transformed to pIC50 and presented as means \pm standard error of the mean (SEM) [159]. Higher values of pIC50 indicated exponentially more potent inhibitors. One-way ANOVA/Kruskal-Wallis test was used to identify differences among pIC50 values of groups, and if a significance was observed, a posthoc analysis was used to locate the difference, i.e. to know which two groups were different (P values <0.05 were considered significant). No data or experiments were excluded from analyses. All statistic analysis above were conducted using IBM SPSS statistic 23 and Prism 8.4. To quantify the protein after performing western blot, pictures were analyzed in Image Studio Ver 5.2.

3 Results

3.1 Information collection of ALK-TKIs resistance spectra with corresponding mutations and fusion variants

To conduct a comprehensive study of ELK4-ALK variants and resistance mutations in ALK, information of co-occurrences of ALK resistance mutations and fusion variants that had already been identified in clinical studies and the corresponding responses to ALK-TKIs was required. Thus, a comprehensive search of two public clinical knowledgebases (CKB CORE [151] and CIViC) was performed. These databases provided five levels of evidence (CIViC score A – E) - indicating the robustness of the study supporting the evidence item - for resistance mutations relevant studies [152]. These levels were:

A validated association, which had a clinical consensus association of the mutation in human medicine;

B clinical evidence, which based on large clinical trials to support the clinical association of the mutation;

C case studies, which had been reported in case reports;

D preclinical evidence, which was supported by *in vivo* or *in vitro* models;

E indirect evidence.

Due to the precision of the information (complete information of ALK mutations, fusion variants and patient responses to ALK-TKIs) required in this work, only studies with level C evidence and partly level D evidence were selected. Moreover, in order to focus on single resistance mutations, reports with incomplete information and those with compound mutations were excluded from this study. Thus, a total of eleven cases with the complete information remained. To stratify patient responses, those with complete response (CR) and partial response (PR) were considered as sensitive, and patients who developed progressive disease (PD) or maintained stable disease (SD) were considered as resistant to ALK-TKIs. An overview of ALK inhibitor resistance spectra including mutations as well as EML4-ALK fusion variants are given in Table 4.

Table 4 Individual responses to ALK inhibitors reported with corresponding ALK mutation and EML4 fusion variant information.

Mutation	Variant	Resistant to	Sensitive to	Level of evidence*
C1156Y	V1	Crizotinib[160]		C
	V3	Ceritinib,Crizotinib[139, 161]	Lorlatinib[161]	C, D
G1269A	V1	Crizotinib[139, 162]	Ceritinib,Alectinib[139, 162, 163]	C, D
	V3	Crizotinib[164]		C
I1171T	V1	Alectinib,Crizotinib[139, 141]		C, D
	V2	Crizotinib[165]		C
	V3	Crizotinib[139]	Ceritinib[139]	D
L1196M	V1	Crizotinib[139, 162]	Ceritinib,Alectinib[162]	C, D
	V2	Ensartinib[166]		C
	V3	Crizotinib[139]	Ceritinib	D
L1152R	V3	Crizotinib[127]		C
G1202R	V1	Crizotinib[139, 140],Ceritinib[167]		C
	V3	Alectinib[168, 169],Crizotinib[161]	Lorlatinib[170]	C

* CIViC evidence level: C-Case study; D-Preclinical evidence

3.2 Construction of expression plasmids encoding EML4-ALK fusion variants with resistance mutations

For the functional testing of different EML4-ALK fusion variants carrying mutations, the commonly used Ba/F3 model was chosen. The Ba/F3 cell line is an immortalized murine bone marrow-derived pre-B cell line [171], it is characterized by the dependence of growth or survive on IL-3. This dependency can be taken over when an active kinase, e.g. EML-ALK fusion, is expressed in these cells. Thus in this context, it is also possible to investigate the activity or efficacy of inhibitors (drug screening).

For this endeavor in a first step, expression plasmids encoding EML4-ALK fusion variants with resistance mutations were cloned. Expression vectors - pCXbsr backbone- encoding EML4-ALK wild type fusion variants V1, V2 and V3a/b were available in the laboratory (Figure 5A, 5B) [153]. Based on the information obtained from clinical studies, involved point mutations were introduced into corresponding fusion variant plasmids by site-directed mutagenesis (Figure 5B). After transformation, bacterial clones were screened by colony PCR (Figure 5C, D) and presence of mutations were confirmed applying Sanger sequencing (done by GATC sequencing service, Figure 5C, D). The plasmid DNA from the confirmed colonies was used in transfections.

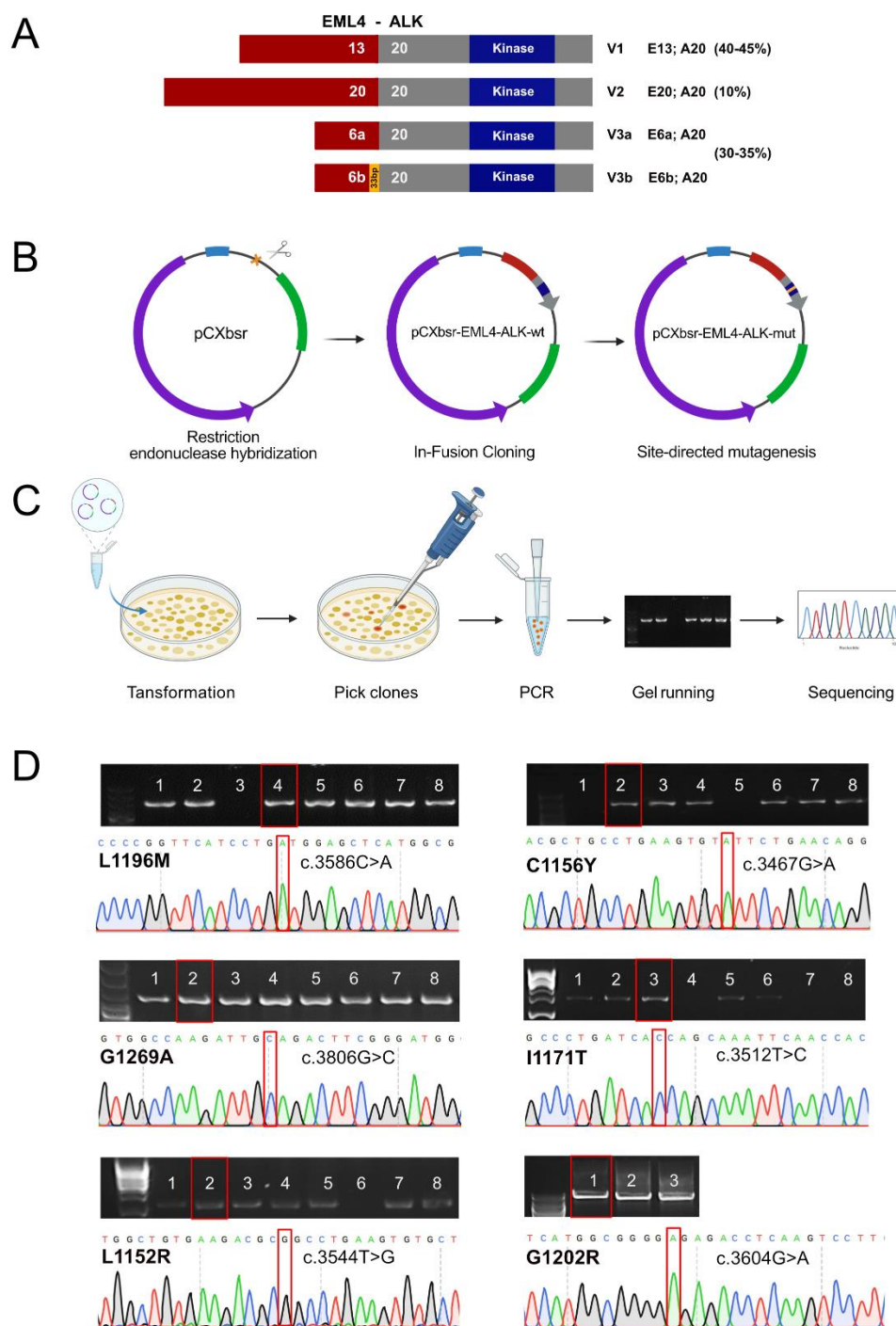


Figure 5 Construction and confirmation of point mutations conferring resistance for ALK specific inhibitors in expression plasmids containing EML4-ALK fusion variants. **A)** Schematic protein structure of the most common EML4-ALK fusion variants. **Red**, EML4 fusion part; **grey**, ALK fusion part; **blue**, tyrosine kinase domain of ALK; **yellow**, 33bp insertion in exon 6 of V3b. **B)** Schematic diagram of the introduction of ALK resistance mutations by site-directed mutagenesis, **C)** confirmation of point mutations by colony PCR and Sanger-sequencing. **D)** Representative DNA sequencing electropherograms confirming successful introduction of point mutations. The sequences of six resistance mutations (L1196M, C1156Y, G1269A, I1171T, L1152R and G1202R) were determined by Sanger-sequencing. Picked clones were marked by red square boxes. **Upper**: gel electrophoreses of colony PCRs. **Lower**: sequencing chromatographs. B and C done with BioRender (www.biorender.com).

3.3 Selecting cell cloning with designed mutations and fusion variants

After successful introduction of resistance mutations into the expression constructs encoding different EML4-ALK fusion variants, plasmids were transfected into Ba/F3 cells applying electroporation in the next step. In order to obtain cells that stably expressed transfected DNA, cells were subjected to a double-selection. ❶ Taking advantage of the addiction of Ba/F3 cells to an activation signal, IL-3 was withdrawn. ❷ Cells were also subjected to blasticidin selection (10-20ng/μl) as the pCXbsr vector encoded a blasticidin S-resistance gene (bsr). Cells surviving this double-selection were subjected to single cell sub-cloning. Four to six clones (Appendix A) were picked from each of the obtained transfected bulks and for proofing correct expression. Cell lysates were subjected to denaturing discontinuous sodium dodecyl sulfate polyacrylamide gel electrophoresis (SDS-PAGE). Levels of phospho-ALK (pALK) and total ALK (tALK) in selected cell clones were determined by Western blotting. Cell clones with comparable expressing of both tALK and pALK were selected for drug screening in subsequent experiments (Figure 6 and Appendix A).

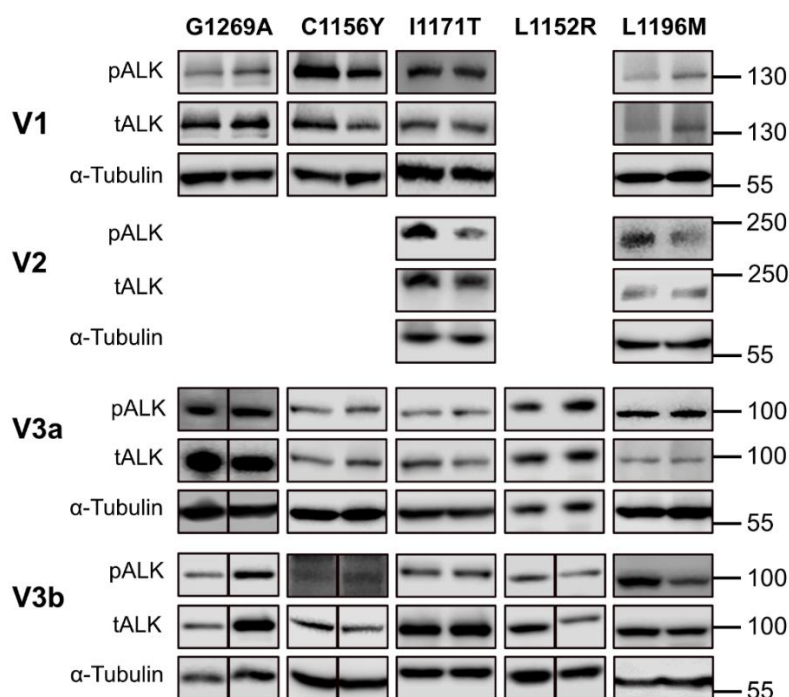


Figure 6 ALK and pALK expression of different mutations in EML4-ALK variants. Western blot tests were performed using antibodies specifically binding pALK (phosphor-ALK), tALK (total ALK) with α -tubulin serving as loading control. Shown are blots with selected and representative cell clones with respective variants and ALK mutations. Details are given in Appendix A.

3.4 Dose selection and cell model reliability assessment

Next, cell viability assays were performed on the Ba/F3 cells expressing mutated EML4-ALK variants. First of all, to warrant specificity which might be spilled by unspecific cytotoxic

effects of different TKIs, Ba/F3 cells transfected with the BCR/Abl fusion (Philadelphia-chromosome) served as negative control in a way that this activated fusion should not be responsive for ALK specific inhibitors. Thus, when Ba/F3 cells expressing BCR/Abl exhibited inhibition, this was taken as a sign of unspecific toxicity, e.g. the highest concentrations of ALK-TKIs (1000nM) reduced cellular activity in BCR/Abl expressing BA/F3 cells, indicating unspecific cytotoxicity (Figure 7A). As a result of this testing, in the following experiments, 250nM of ALK specific inhibitors was used as the maximum concentration in cell viability assays as it did not cause unspecific cytotoxicity.

Although Ba/F3 cells is a popular model system for assessing activity of small molecule kinase inhibitors in target therapy, it remained unknown if it was also reliable in the present study, i.e. if the activity of ALK-TKIs against mutations tested in Ba/F3 cells was consistent with patient response reported in clinical studies (Table 4, Figure 7C). To quantify responses of cells to ALK-TKIs, cell viability altered along with serial diluted ALK-TKIs was calculated and indicated by IC50 or pIC50. Lower values of IC50 and higher values of pIC50 indicated – exponentially - higher potency of an inhibitor. In addition, ROC curves were used as a graphical approach to show the diagnostic capability of binary classifiers. It allowed, on the one hand, to find the appropriate classification threshold for used inhibitor and, on the other hand, to assess the performance of the inhibitor under investigation by a binary classification algorithm applying AUC (area under the curve) calculations. As patients' responses to ALK-TKIs were divided into two categories: ❶ sensitive and ❷ resistant, the continuous variables (IC50 or pIC50) obtained from cellular model were accordingly convert into the dichotomous variables: ❶ sensitive and ❷ resistant (see also 3.1) by ROC curve, which making it possible to map experimental results from cell culture with patients' responses. And in this setting, the best cut-off point pIC50 value of 7.339 was defined to distinguish sensitive (>7.339) and resistant (<7.339) cells to ALK-TKIs. All cell viability tests were converted to sensitive- and resistant-group and mapped to patients' responses in clinical reports. If a patient with a specific ALK-fusion and mutation combination was reported to be resistant to a TKI and the corresponding cellular assay also categorized as resistant, they were considered to be matched or if not as unmatched. Altogether, 34 out of 37 (91.9%) cellular tests matched with cases (Figure 7C). Moreover, ROC curve modelling also indicated an outstanding diagnostic ability of the cellular model in this study with an AUC value of 0.917 (Figure 7B). In conclusion, both of ROC curve and report-model mapping plots suggested that the Ba/F3 models in the current study provided reliable results reflecting the clinical responses to ALK-TKIs.

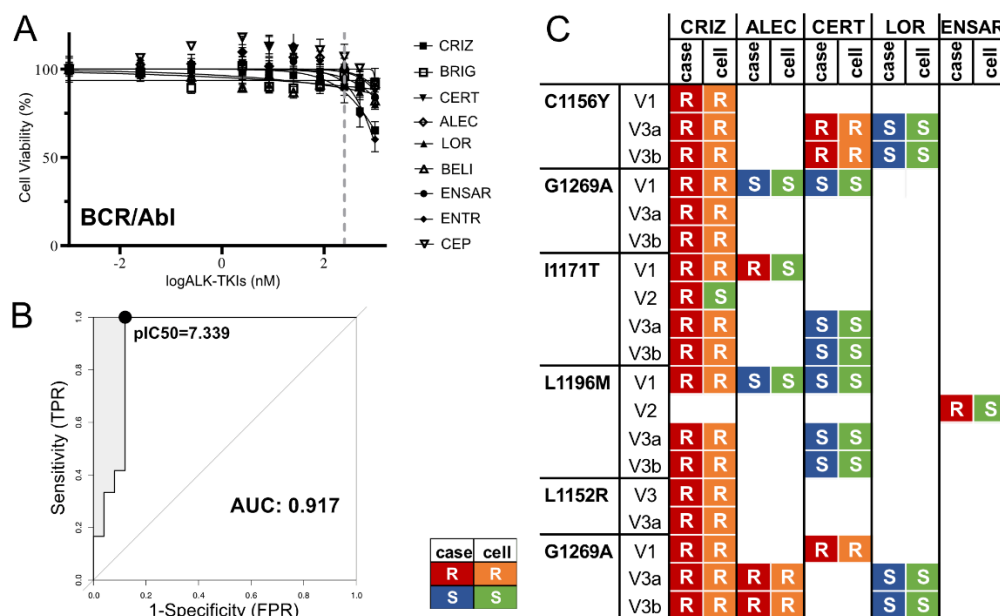


Figure 7 Dose selection and cell model reliability assessment. **A)** Sensitization of Ba/F3 cells expressing BCR/Abl by treatment with nine ALK-TKIs. Cells were treated with the indicated doses of ALK-TKIs for 48 hours and followed by cell viability assay using the alamarBlue viability assay (alamarBlue™). Values are presented as means (N = 3). **Grey dash line** indicate the highest concentration that did not cause unspecific cytotoxicity. **B)** ROC curve evaluating the reliability of cell models for predicting responses of mutations and variants to ALK-TKIs. **Black dot**, best cut-off. **C)** Report-model mapping plot of investigated mutations and fusion variants. Resistance to indicated inhibitors is given for patients in **red**, when case was reported as resistant, **blue**, when being sensitive and for cells in **orange**, when being resistant, or **green**, when being sensitive.

3.5 Activity of ALK-TKIs in different combinations of resistance mutations and fusion variants

After proving the reliability of the cellular models in this study, they were further applied to cell viability tests in all ALK-TKIs. In total, the following nine ALK-TKIs were chosen for drug screening: ❶ first-generation TKI crizotinib, ❷ second-generation TKIs ceritinib, alectinib and brigatinib, ❸ third-generation TKI lorlatinib, and ❹ entrectinib, ensartinib, belizatinib and CEP-37440, which have not been approved for treatment of ALK-positive NSCLC patients but showed inhibitory activities against activating ALK rearrangements in both preclinical and clinical studies (Table 3).

According to the threshold gained from the ROC curves for distinguishing sensitive and resistant groups, all measured IC₅₀ and pIC₅₀ values were categorized into three groups: ❶ absolute resistant group (mean pIC₅₀+SD <7.339), ❷ the absolute sensitive group (mean pIC₅₀-SD >7.339) and ❸ intermediate group (mean pIC₅₀-SD <7.339, mean pIC₅₀+SD >7.339) (Figure 7B, Table 5 and Appendix B). According to this scoring system, cells with EML4-ALK fusions and the following mutations displayed strong sensitivity for ALK specific inhibitors:

- L1196M - ceritinib, alectinib, brigatinib, lorlatinib and belizatinib
- I1171T - ceritinib, alectinib, brigatinib, lorlatinib, belizatinib and ensartinib
- C1156Y - alectinib, brigatinib, lorlatinib ,belizatinib and ensartinib
- G1269A - ceritinib, alectinib, brigatinib, lorlatinib, belizatinib and CEP-37740
- L1152R - alectinib, brigatinib, lorlatinib, belizatinib, entrectinib and ensartinib.

An intermediate sensitivity was seen for

- G1202R - lorlatinib.

As expected, the third-generation ALK-TKI lorlatinib, which was designed for targeting mutations that were resistant to first- and second-generation ALK-TKIs, exhibited efficacy against all tested ALK mutations, especially including G1202R mutation (Table 5, Figure 8, and Appendix B). However, lorlatinib was not the most potent inhibitor for all mutations. Namely, lorlatinib showed the greatest activity against I1171T, G1202R and C1156Y mutations, while brigatinib was the most potent inhibitor for L1152R mutations and belizatinib was for L1196M. Alectinib, brigatinib and belizatinib also potently inhibited ALK phosphorylation across all mutations and fusion variants except G1202R. Ceritinib was inactive against C1156Y and L1152R mutations. These results indicated that in addition to lorlatinib, more potent ALK-TKIs targeting to different ALK resistance mutations might be selected.

Concerning different sensitivities mediated by distinct fusion variants, the activities of various ALK-TKIs against V1, V2 and V3a/b variants of ALK resistance mutations were also evaluated (Table 5, Figure 8). In general, cell viabilities in V3a and V3b did not differ significantly in the various mutations. An exception of this observation was seen in cells with EML-ALK fusions and I1171T or G1202R mutations. Here, V3b conferred more cellular resistance compared with V3a when treated with CEP-37440 ($p=0.022$ and $p=0.012$, respectively, Figure 8). Moreover, V1 was more sensitive than V3a/b in EML4-ALK with G1202R and G1269A mutations, but the opposite was observed in the context of L1196M, I1171T or C1156Y mutations. Specifically, V1 mediated significantly higher resistance compared with V3a, not V3b, in the presence of L1196M mutations against ceritinib ($p=0.007$), entrectinib ($p=0.043$) and CEP-37440 ($p=0.043$); I1171T mutations with ceritinib ($p=0.002$) and belizatinib ($p=0.002$); and C1156Y mutations with lorlatinib ($p=0.016$). Only in the context of a C1156Y mutation, V1 mediated significantly higher resistance compared with V3b for crizotinib ($p=0.035$), belizatinib ($p=0.036$) or CEP-37440 ($p=0.04$). An opposite behavior was observed for I1171T mutations in EML4-ALK V1 and V3a/b with lorlatinib ($p=0.021$), G1202R with alectinib ($p=0.004$) and CEP-37440 ($p=0.041$), G1269A with brigatinib ($p=0.011$) and lorlatinib ($p=0.021$). V2 variant was only reported and established with L1196M and I1171T mutations (Figure 7C). Both mutations were more susceptible for all

ALK-TKIs except I1171T with CEP37440 compared to other variants. In total, a tendency was observed in the cell viability assays that V2 was most sensitive followed by V1 and V3b, whereas V3a was least sensitive to all tested ALK specific inhibitors. In addition, although in general, effects of fusion variants and mutations seemed cumulatively affecting cell's responses to a certain inhibitor, there were exceptions: in cells harboring L1196M mutation, V1 conferred higher resistance to lorlatinib than V2 or V3a, while I1171T mutations rendered V1 transfected cells more sensitive to lorlatinib than V2 or V3a, which was not in line with other inhibitors and mutations.

In summary, the cell viability assays showed that even though differences in the tested fusion variants could affect cell sensitivity to ALK-TKIs, the specific ALK-inhibitor affected cellular activity mostly. It turned out that brigatinib gave the best responses for G1269A- and L1152R mutations, lorlatinib for C1156Y and I1171T mutations, and belizatinib for G1269A and L1196M mutation.

Table 5 Mean IC50 (nM) of different ALK-TKIs on cellular ALK phosphorylation in Ba/F3 cells harboring differing EML4-ALK variants with C1156Y-, L1196M-, G1269A-, I1171T-, L1152R- or G1202R-mutations. **Green-** and **red wells** indicate absolute sensitivity or resistance, respectively, **yellow wells** intermediate sensitivity or resistance, and **dark green wells** mark the most potent inhibitors for the corresponding mutation-fusion combinant. CRIZ, crizotinib; CERT, ceritinib; ALEC, alectinib; BRIG, brigatinib; LOR, lorlatinib; BELI, belizatinib; ENTRE, entrectinib; ENSAR, ensartinib; CEP, CEP-37440. Table of pIC50 with SD shown in Appendix B.

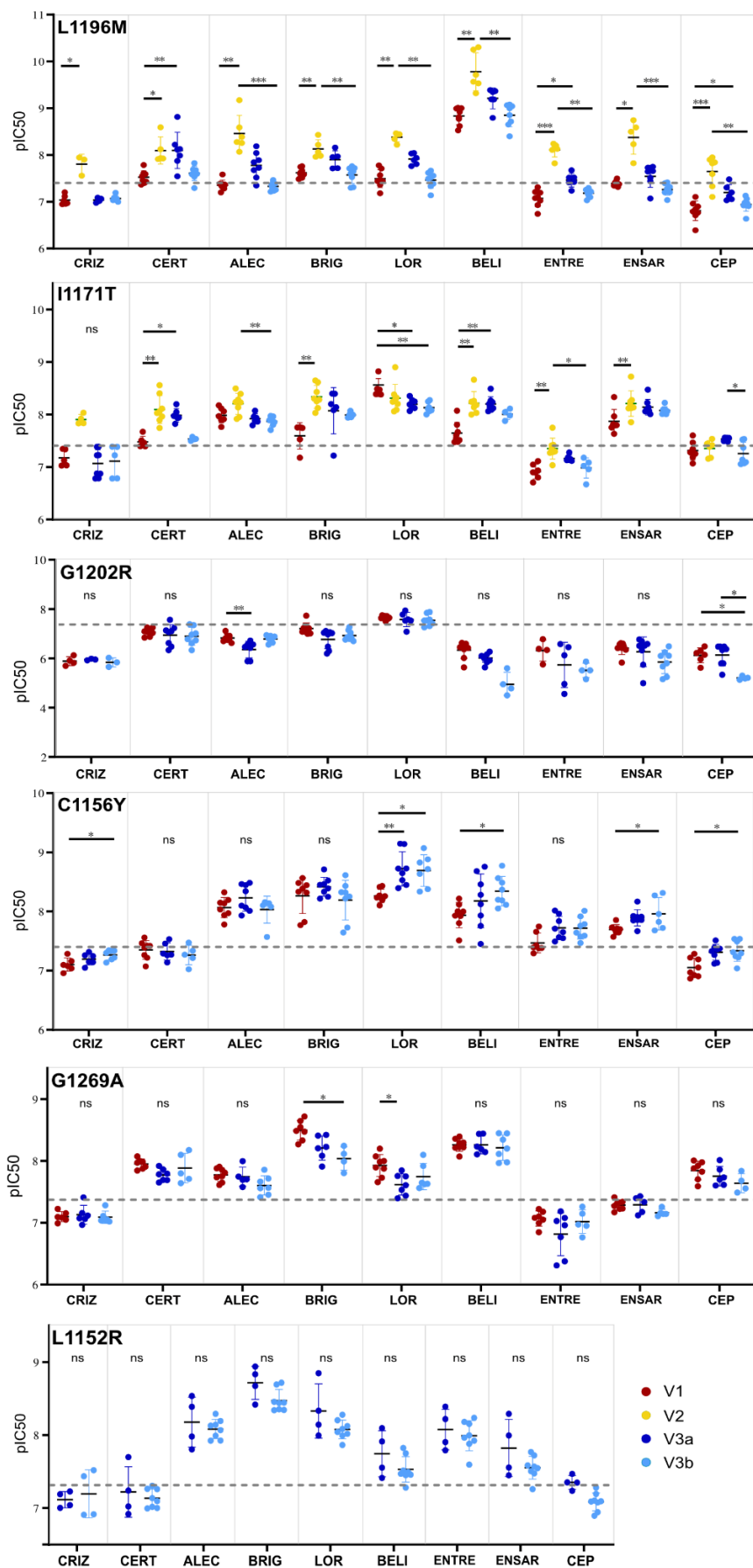
Mutations	Variants	Cellular ALK phosphorylation mean IC50 (nM)								
		CRIZ	CERT	ALEC	BRIG	LOR	BELI	ENTRE	ENSAR	CEP
C1156Y	V1	78.93	44.68	8.60	5.43	5.46	11.55	34.09	20.18	83.91
	V3a	64.06	47.44	5.89	3.83	1.91	6.62	18.96	12.84	49.15
	V3b	54.25	54.63	9.31	6.44	2.03	4.55	19.12	10.95	46.40
G1269A	V1	79.80	11.23	16.83	3.19	11.87	5.53	85.70	51.89	14.38
	V3a	74.25	16.99	18.05	6.19	24.13	5.52	153.39	51.23	17.66
	V3b	81.41	13.06	24.94	6.77	17.96	6.13	95.98	69.12	22.91
L1196M	V1	92.23	30.00	44.19	24.00	32.15	1.48	84.66	40.82	155.84
	V2	15.79	8.04	3.48	7.41	4.16	0.17	7.79	4.20	22.50
	V3a	92.20	7.99	16.67	12.55	12.26	0.62	34.51	28.68	63.55
	V3b	85.33	24.64	46.96	26.76	34.44	1.41	65.59	54.85	114.71
I1171T	V1	66.97	33.10	10.36	25.52	2.61	22.62	122.15	13.50	48.52
	V2	12.42	8.02	6.23	4.61	4.88	5.06	44.61	6.19	44.49
	V3a	85.60	10.35	12.06	8.46	6.32	6.29	68.23	7.23	29.38
	V3b	77.19	29.23	13.45	10.21	7.40	9.89	104.09	8.37	55.62
L1152R	V3a	76.75	60.31	6.65	1.93	4.68	18.03	8.40	15.06	44.53
	V3b	63.87	73.45	8.27	3.36	8.39	29.51	10.20	27.95	82.31
G1202R	V1	1188.98	83.34	144.58	60.43	21.71	449.18	469.69	374.66	728.86
	V3a	1077.11	111.49	519.91	164.97	26.10	254.34	1654.79	352.09	710.43
	V3b	1398.11	123.79	159.73	115.40	27.89	48398.66	1827.08	1499.06	5843.75

sensitive

intermediate

resistant

RESULTS



(Legend on next page)

Figure 8 Inhibition efficacy of different ALK-TKIs against Ba/F3 cells harboring various EML4-ALK fusion variants and L1196M-, I1171T-, G1202R-, C1156Y-, G1269A- or L1152R mutations. Ba/F3 cells were treated with the indicated ALK-TKIs for 48 h. Scatter plots of pIC50 calculated from viability analysis using alamar blue assay. **Red** dots represent variant 1 (V1), **yellow** variant 2 (V2), **dark blue** variant 3a (V3a) and **light blue** variant 3b (V3b). **Grey lines** indicate best cut-off of separating samples into resistant- and sensitive-groups. Each dot indicates an independent sample examined and data are presented as mean values \pm SD. Groups were compared by Kruskal-Wallis- together with Bonferroni post hoc tests. *, $p < 0.05$; **, $p < 0.01$; ***, $p < 0.0001$; ns, not significant. CRIZ, crizotinib; CERT, ceritinib; ALEC, alectinib; BRIG, brigatinib; LOR, lorlatinib; BELI, belizatinib; ENTRE, entrectinib; ENSAR, ensartinib; CEP, CEP-37440.

3.6 Belizatinib is the most potent inhibitor of EML4-ALK fusion proteins with L1196M mutation

From the drug screening experiments for cellular activity, targeted ALK-TKIs for different mutations were identified, of which the most interesting was the inhibitory capacity of belizatinib to EML4-ALK variants with an L1196M mutation (ALK-L1196M) because belizatinib was approximately twenty times as potent as lorlatinib in ALK-L1196M, regardless of the fusion variants (Table 5, Appendix B).

To further clarify whether the potent inhibitory efficacy of belizatinib against ALK-L1196M was due to its specific targeting effect to ALK, the level of phosphorylated ALK were assayed after the addition of belizatinib. The first generation inhibitor crizotinib and the third generation inhibitor lorlatinib served as control. Shown by Western blot, levels of phosphorylated ALK (pALK) were decreased in a dose-dependent manner in all fusion variants (Figure 9B, C). At a concentration of 30mM, belizatinib completely suppressed the viability of L1196M-expressing cells in all variants, while crizotinib and lorlatinib did not. This was supported by levels of phosphorylated ALK which were consistent with the cellular results indicated by IC50-levels (Figure 9A). In addition, pALK levels remained constant in V1 and V3b at the concentration of 300nM crizotinib, but decreased in V3a and disappeared in V2. Lorlatinib inhibited ALK phosphorylation of V3a/b and V2 at concentrations of 30nM and V1 at 100nM, respectively. Phosphorylation levels differed in variants under the same concentration of TKIs again confirming the previous conclusions that V2 showed highest sensitivity to ALK-TKIs. Thus, the robust efficacy of belizatinib could be attributed to a specific targeting effect of ALK-specific inhibitors for ALK-L1196M.

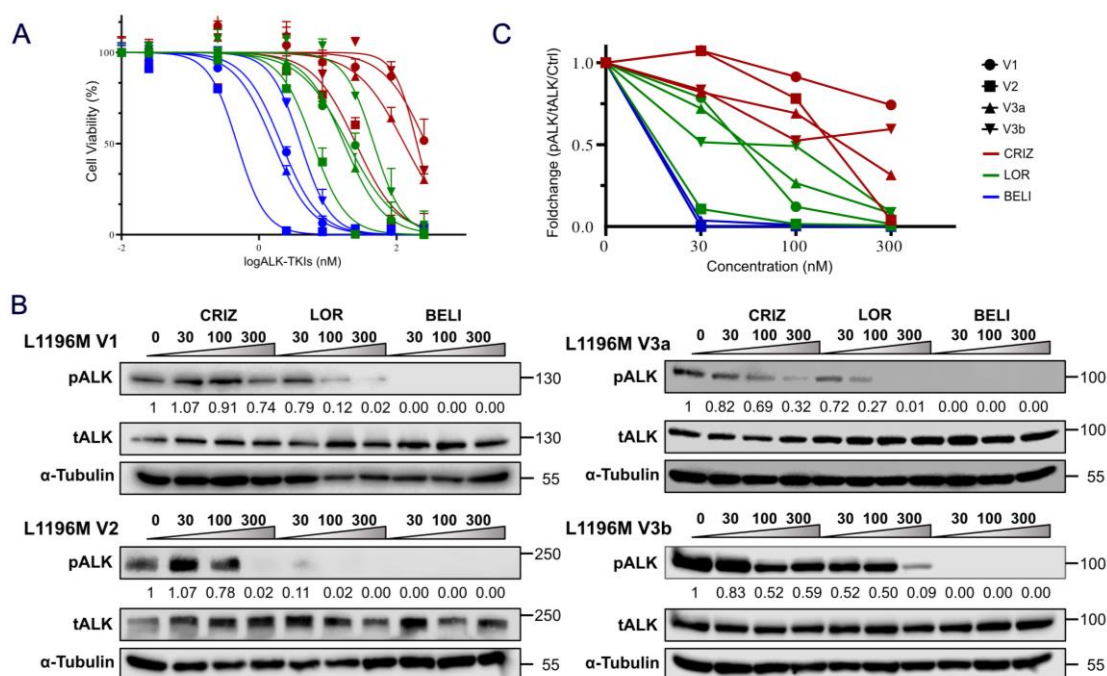


Figure 9 Effect of crizotinib, lorlatinib and belizatinib on ALK phosphorylation in different EML4-ALK fusion variants with L1196M mutation. **A)** IC₅₀ curves of ALK-L1196M mutation in EML4-ALK variants V1, V2, V3a and V3b treated with crizotinib, lorlatinib and belizatinib. **Symbols** indicate variants. **Round**, V1; **square**, V2; **upright triangle**, V3a; **downward triangle**, V3b. **Color of lines** indicate ALK-TKIs. **Red**, crizotinib; **green**, lorlatinib; **blue**, belizatinib. **B)** Western blot analysis of phospho-ALK (pALK) in cells treated with crizotinib, lorlatinib and belizatinib. Cells were cultured at indicated concentrations of ALK-TKIs for 3 hours. **C)** Relative levels of ALK phosphorylation. Values were analyzed by quantified densitometrically as the ratio of pixel intensity of indicated bands of pALK to total ALK amounts (tALK). All values are normalized by DMSO control group (0mM inhibitor). Color of lines and symbols show the same as A). CRIZ, crizotinib; LOR, lorlatinib; BELI, belizatinib.

3.7 Increased compound–protein interactions (CPIs) contribute to the sensitivity of ALK-L1196M to belizatinib

Next, efforts were taken for understanding the possible molecular mechanisms for the strong inhibitory efficacy of belizatinib. Molecular docking [6] (MD) is a key tool in computer-assisted drug design (CADD) for probing inhibitor-protein binding modes and protein conformational changes. It could propose structural hypotheses on how ligands inhibited their targets. In order to get a better impression of the structure-function relationship of belizatinib and ALK-L1196M kinase domain complex, molecular docking was performed using Autodock. As a source of 3D structural data, the protein database (PDB) was used. PDB contains many 3D models obtained by X-ray crystallography or other methods. For the current project the X-ray conformation of belizatinib binding with ALK-WT (PDB ID: 4fod) was downloaded from PDB. First of all, the chosen approach for calculating molecular docking should be proven to warrant that the chosen approach was valuable. Therefore, the bound ligand, belizatinib in

4fod, was fetched from the complex and submitted to redock into ALK-WT (PDB ID: 6cdt) employing Autodock. The best-scored geometry, named BELI-ALK-WT bound conformation, was then picked to compare with the bound X-ray conformation (4fod), and the difference between them was shown by root-mean-square deviation of atomic positions (RMSD), a measurement of the accuracy of the predicted conformation. With a RMSD of 0.403Å (for ligand docking RMSD < 2Å is good, RMSD < 1Å is very good [172]) (Figure 10A), the protein–ligand docking program and docking parameters used in the current study were indicated reproducible and reliable thereby validating the chosen approach.

After this validation step, same approach was performed in a second step on belizatinib and ALK-L1196M. Again, the best-scored conformation (BELI-ALK-L1196M) was chosen and compared with BELI-ALK-WT. As shown in the MD models, the binding sites of belizatinib in ALK-WT and ALK-L1196M were both located in the flat pocket defined by Val1180 and Leu1256 between the N- and C-lobe (Figure 10A, 10B), which is also the binding site for ATP (Figure 3). However, the binding site of belizatinib in BELI-ALK-L1196M compared to that of belizatinib in BELI-ALK-WT was deeper in the pocket and closer to the hinge residue, which usually interacts with most of the small molecule inhibitors of protein kinases by forming hydrogen bonds [142]. Moreover, three hydrogen bonds were predicted by the MD model: ❶ an NH-group of the benzimidazole ring of belizatinib formed a hydrogen bond to Ala1200O, ❷ an oxygen in the carbonyl-residue of the benzoyl-group in belizatinib formed a hydrogen bond with Glu1197O and ❸ Met1199N, respectively, in the hinge residue (Figure 10B). In contrast, the binding site of belizatinib in BELI-ALK-WT was located far away from the hinge residue, and was therefore not able to form hydrogen bonds with the hinge residue (Figure 10B), indicating a lower compound-protein interaction. Considering the reason for these changes may be the replacement of leucine by a methionine in ALK-L1196M, which increased the depth of the pocket spatially, and therefore provides a moderate distance for hydrophobic interactions between belizatinib and ALK-L1196M. In support with the results from the MD model, belizatinib showed an increase activity in ALK-L1196M compared to that in ALK-WT (Figure 11).

In conclusion, the CPI might be a major factor influencing the activity of small molecular inhibitors [158, 159], and the data represented in this thesis support a higher binding strength and thus efficacy of belizatinib in the interaction with ALK-L1196M what is explained by an enhanced CPI.

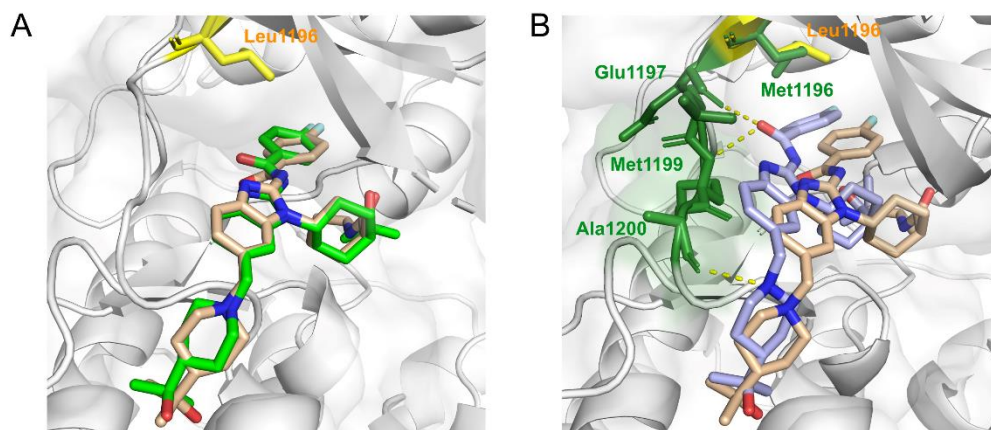


Figure 10 Predicted compound-protein interactions of belizatinib and ALK-WT or ALK-L1196M, respectively. **A)** Comparison of the predicted geometry of belizatinib and that of in X-ray crystal derived ALK-WT model. **Light green**, belizatinib geometry of X-ray crystal (PDB ID: 4fod). **Wheat**, belizatinib geometry of predicted conformation in ALK-WT. **Yellow**, Leu1196 in ALK-WT. **B)** Comparison of predicted geometry of belizatinib in ALK-WT and ALK-L1196M. **Wheat**, belizatinib geometry of predicted conformation in ALK-WT. **Purple**, belizatinib geometry of predicted conformation in ALK-L1196M. **Yellow**, Leu1196 in ALK-WT. **Green**, amino acids highlight in ALK-L1196M, namely Met1196, Glu1197, Met1199 and Ala1200. Docking structures were visualized using PyMOL and are shown by grey colored surface, sticks, helices and ribbons (**N**, blue; **O**, red; **Cl**, green; **F**, light blue). **Dash lines** indicate hydrogen bonds between residues of protein and inhibitor.

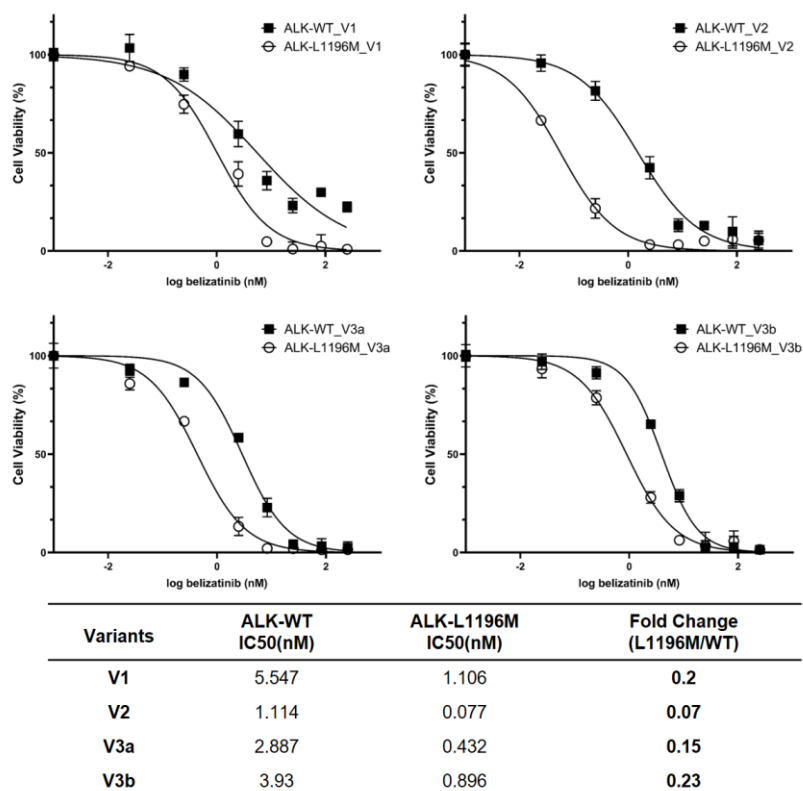


Figure 11 IC₅₀ of Ba/F3 cells harboring ALK-WT and ALK-L1196M by treatment with belizatinib. Cells were treated with the indicated doses of belizatinib for 48 hours and followed by cell viability assay using the alamarBlue viability assay. **Solid square**, IC₅₀ curve of ALK-WT to belizatinib; **empty circle**, IC₅₀ curves of ALK-L1196M to belizatinib.

4 Discussion

For a comprehensive drug-response study of different mutations in EML4-ALK fusion variants, 37 combinations of clinically reported ALK-resistance mutations and fusion variants were selected for drug screening using cellular models in this study. This selection warranted that only clinically relevant combinations of fusion-variant and mutation were tested. Moreover, although Ba/F3 cells are commonly used for drug screening [173], their accuracy in this study still needs to be confirmed. By conducting ROC curve with pIC50 values measured by cell viability tests, all tests were converted to two groups: sensitive and resistant, and further mapped to patients' responses in clinical reports. All together, the cellular models used in the current study indicated as an outstanding diagnostic ability with an AUC value of 0.917. 34 out of 37 (91.9%) tests matched with cases but three (8.1%) did not. One of the cases failed in matching was a patient progressed under alectinib treatment for four months and the I1171T mutation was detected in a rapidly fresh frozen tissue sample [141]. For this patient, cell viability assays were done using ① H3122 cells – an EML4-ALK WT cell line, ② MGH056-1 – patient derived cell line with I1171T mutation in EML4-ALK, and ③ H3122 CHR-A1 – generated by long-term incubation with alectinib but with unknown mutation. The author concluded MGH056-1 cells, which harbored I1171T mutation, had intermediate resistance to alectinib by comparing to other two cell lines although there were different factors affecting the results, namely cells of different origins, cells with unknown mutations. In contrast, the data present in the current study are discussed in a scientific way, i.e. only one parameter was compared among cells. In this context, the results in this study are more convincing. Both of the other two unmatched cases were mutations in V2 structure, they were I1171T mutation to crizotinib and L1196M mutation to ensartinib in V2 [165] [166]. Although V2 has been suggested to be the most sensitive variant compared to V1 and V3 by preclinical or small cohort studies [68, 133], which was supported my results, due to small sample sizes and too less information was reported, no statistic significant conclusion can be drawn. And for sure further investigations with larger cohort and more cases are needed to clarify the sensitivity of mutations in the context of V2.

Notably, unlike previous clinical or preclinical studies, pIC50, the negative log of the IC50 value, was used as the efficacy evaluation of ALK-TKIs for comparison in this study. Considering that dose dependent inhibition of cells is a logarithmic phenomenon, pIC50, the logarithmic scale of IC50 has the nature of normal distribution, can provide an adequate and thus better way to calculate arithmetic mean values and standard deviations, while IC50 cannot. However, in order to make it easier to compare the values with those of other studies, data of this study was presented with both IC50 and pIC50 values. In addition, ROC curve analysis was also established in the current study for assessing whether and how well pIC50 was capable of predicting the patients' responses with certain mutation-fusion combination

to ALK-TKIs. Interestingly, pIC50 of 7.339 was calculated as the best cut-off point to distinguish between sensitive and resistant responses, and the cell model proved excellent with an AUC of 0.917. Taken together, although no such correlation has been established for ALK-TKIs or other targeted inhibitors before, in this study the reliability of the cell model was verified, and the correlation between pIC50 and responses to ALK-TKIs has been well established.

Although most NSCLC patients with ALK-gene fusions initially responded to different generations of ALK-TKIs, but patients ultimately relapsed within 1-2 years due to distinct resistance mechanisms [79, 80, 90, 95, 174, 175]. One of the most common mechanisms is the occurrence of drug resistance mutations in the *ALK* gene, so-called on-target resistance mutations, which, on the one hand, preserve and facilitate the ALK signaling pathway activity (in pathway resistance mutation) [85, 108], and on the other hand interfere the binding of ALK-TKIs into the ATP-binding pocket [85, 176]. For example, the L1196M gatekeeper mutation affects the flexibility of the P-loop (residues 1223-1228, Figure 1), which mediates the proper localization of ATP, thereby increase the interaction of ATP with ALK, and further strongly influence the ALK-crizotinib interaction [177]. In addition, the gatekeeper residue locates near the top of the regulatory spine (R-spine) and modulates the spine. The replacement of leucine with methionine (L1196M) may enhance the homeostasis of R-spine and thus favor the activity of ALK, which is proved by greater cellular baseline levels of phosphorylation of ALK in L1196M mutation than in wild type [85, 108]. Unlike L1196M mutation, the solvent frontier G1202R mutation leads to spatial conflict with the piperidine ring of crizotinib due to the increased size of the arginine (R) residue in the mutated molecule [176], which is also spatially blocked from the large and rigid tetra-substituted phenyl group in ceritinib [139], and thus both TKIs are inactive against the G1202R mutation.

In terms of the development process of ALK inhibitors, second-generation inhibitors were designed to overcome crizotinib resistance mutations [70, 178, 179], and lorlatinib was developed from crizotinib and specifically designed to target mutations that are resistant to crizotinib and the second-generation TKIs [78, 180, 181]. It is therefore often assumed that the new generation of inhibitors will be more effective than the previous generation. But the emerged lorlatinib resistance mutation, L1198, which re-sensitized tumors to crizotinib, highlighted the complexity of the emerging ALK resistance mutations. Consistent with these results, cell viability assays in this study showed that second-generation TKIs were more effective against crizotinib-resistant mutations, and that the third-generation TKI lorlatinib had better activity against ceritinib-resistant mutations C1156Y and L1152R. However, in addition to this, this present study concluded that a purely sequential approach of first-, second- and third-generation therapy might not provide the best therapeutic benefit, and that a targeted sequential approach to different mutations might result in a higher benefit to patients. Taken together, this suggested that patients with NSCLC driven by ALK-gene fusion who develop

resistance might benefit most by administering an appropriate ALK-TKI with the highest efficacy for the present resistance mutation.

Effects of ALK-TKIs on NSCLCs carrying ALK resistance mutations have been widely investigated in several studies [133] [68] [135-137], but there still remains controversy about whether to include also EML4-ALK variants into clinical diagnosis as reports are conflicting regarding whether variants affect response to inhibitors. A retrospective analysis reported that the 2-year progression-free survival (PFS) rate was higher in patients with V1 and V2 (69%) who received generation inhibitors than patients with V3a/b (32.7%) [68]. In line with that, the efficacy of crizotinib as a first-line treatment to EML4-ALK variants patients, higher PFS was found in patients with EML4-ALK variants 1 (11.0 months) than patients with other variants (4.2 months) [182]. Some preclinical studies also indicated that distinct sensitivity of NSCLC cells to ALK-TKIs is associated with difference in protein stability of EML4-ALK [133]. However, contrast to those studies, no significant difference of mPFS among V1, V3a/b and other ALK variants has been reported [136], and similar results also observed that objective response rates to crizotinib, ceritinib or alectinib were similar among “short” variants (V3a/b, V5a/b), “long” variants (V1) and other ALK translocations [135]. A recent systematic review and meta-analysis evaluated 1903 cases of ALK-positive NSCLC patients in 39 studies. It showed that the ORRs of crizotinib was not significantly different between patients with V1, V2 or V3 [183]. Several reasons might be considered for this set of contradictionary results. First, parameters were not uniform. For example, ❶ the classifications of groups under comparison were different, such as long variant vs short variant, V1 vs non-V1, or V1 and V2 vs V3; ❷ the assessment of patient response was based on different criteria, such as PFS, mPFS or ORR, etc.; ❸ patients were treated with different ALK-TKIs, such as crizotinib or other-generations of inhibitors. Second, differences in the frequency of EML4-ALK variants were significant. The prevalences of V1, V2 and V3 are around 40.38%, 6.59% and 26.54%, respectively [183], which may exacerbate the statistic limitation due to small sample size of V2. Third, the existing studies are mainly in vitro studies or small-size retrospective studies. There are no large-scale multicenter studies or prospective clinical studies. Thus, these studies are each by its own too small to draw systematic conclusions in the context of effects of variants, and therefore indicating again the sense and use of larger powered studies which lead to significant results.

Due to the diversity in ALK mutations, the distinct efficacy of ALK-TKIs and the uncertain effects of fusion variants, these pose challenges in terms of selecting the best treatment for patients. This study therefore tried to identify the optimal treatment through ❶ a broad panel of ALK-TKIs against ❷ single resistance mutations ❸ in the context of different EML4-ALK fusion variants. Results from this study showed a tendency in the cell viability assays that V2 was most sensitive to ALK-TKIs, V1 and V3b had intermediate sensitivity and V3a was least sensitive. This is supported by others [133] indicating that differences among EML4-ALK

variants were due to the stability of different fusion-proteins, mostly affected by the N-terminal structure and the variable EML4 part of EML4-ALK fusion proteins. The longest variant (V2), which contained TD-, basic-, HELP-motif and incomplete TAPE domain, was the least stable but most sensitive variant to ALK inhibitors; and the shorter V3a/b, which only contained TD- and basic-motif, was most stable but with a lower sensitivity. However, as shown by the cell viability assays in the current study, although differences in fusion variants affected cell sensitivity to inhibitors, it was the choice of TKI that played the decisive role in influencing cell activity.

Based on a drug screen for cellular activity, this study gave recommendations for the most optimal treatment for patients with diverse mutations or ALK-fusion variants. Belizatinib was among the most noteworthy inhibitor, as it was approximately twenty times as potent as lorlatinib in EML4-ALK-L1196M, regardless of the type of fusion variant. Remember that belizatinib is a known potent inhibitor of both ALK and TRKA/B/C. In a phase I clinical trial using belizatinib (TSR011) [113], it was demonstrated that this drug is characterized by a favourable safety profile but limited clinical activity. Thus the further development was discontinued. However, the present study demonstrated that belizatinib exerts distinct activities in the context of different mutations, for instance, the L1152R mutation generated tolerance to belizatinib, G1269A and C1156Y mutations showed intermediate sensitivities, while L1196M mutation was extremely sensitive to belizatinib ($IC_{50} < 1.5nM$). Therefore, it may be considered that belizatinib might be a useful drug when it comes to a specific targeting for distinct mutations, such as L1196M or G1269A, rather than choosing widely used therapeutic agents, which have been approved for ALK-fusion positive patients with NSCLC.

Furthermore, in an effort to find the mechanistic explanation of the distinct activities of ALK-TKIs in diverse mutations, MD models resulted in a rationale that the L1196M mutation providing space for belizatinib binding and allowing an enhanced belizatinib-ALK-L1196M interaction. Due to an enhancement of the distance of sidechains in both ALK-kinase and belizatinib, hydrophobic interactions might be enhanced resulting in highly stable interaction and thus efficacy, which was further suggested by a higher efficacy of belizatinib in ALK-L1196M compared to ALK-WT. Taken together, these results provided a molecular explanation for the potent effect of belizatinib on L1196M mutations, suggesting that belizatinib might be a better to optimal option for sequential therapy of patients with EML4-ALK L1196M mutation. Given that L1196M is the most common ALK resistance mutation in NSCLC patients [70], the importance of this finding becomes significant.

This study was designed as a systematic research approach. The joint construction of EML4-ALK variants and mutations in this experiment is a technical verification that might be used for a general quick inhibitor screening for any newly emerging variants or mutations in the future, in order to set up more and better-individualized therapy plans. Currently, only single

mutations were included in this study, but as multiple mutations are becoming gradually common because of an accumulating effect after several lines of treatments [161, 169, 184-188], in future studies, multiple mutations in different fusion variants may also be of interest. In addition, tumor resistance is affected by multiple factors. Although this study confirmed the reliability of the cellular models, additional *in vivo* studies and supporting data from clinical trials are still needed.

In summary, this study provides the inhibitor efficacy spectra with clinical confirmed EML4-ALK mutation-fusion combinations to nine ALK-TKIs and offers an optimal sequence of ALK-TKIs for ALK-positive patients carrying resistance mutations. Notably, this study showed that belizatinib might be a promising specific inhibitor for targeting the L1196M mutation of EML4-ALK in NSCLC.

5 References

1. Herbst, R.S., D. Morgensztern, and C. Boshoff, *The biology and management of non-small cell lung cancer*. Nature, 2018. **553**(7689): p. 446-454.
2. Carioli, G., et al., *European cancer mortality predictions for the year 2021 with focus on pancreatic and female lung cancer*. Ann Oncol, 2021. **32**(4): p. 478-487.
3. Jemal, A., et al., *Global cancer statistics*. CA Cancer J Clin, 2011. **61**(2): p. 69-90.
4. Raso, M.G., N. Bota-Rabasedas, and Wistuba, II, *Pathology and Classification of SCLC*. Cancers (Basel), 2021. **13**(4).
5. Rossi, A., et al., *Carboplatin- or cisplatin-based chemotherapy in first-line treatment of small-cell lung cancer: the COCIS meta-analysis of individual patient data*. J Clin Oncol, 2012. **30**(14): p. 1692-8.
6. Sundstrom, S., et al., *Cisplatin and etoposide regimen is superior to cyclophosphamide, epirubicin, and vincristine regimen in small-cell lung cancer: results from a randomized phase III trial with 5 years' follow-up*. J Clin Oncol, 2002. **20**(24): p. 4665-72.
7. Takada, M., et al., *Phase III study of concurrent versus sequential thoracic radiotherapy in combination with cisplatin and etoposide for limited-stage small-cell lung cancer: results of the Japan Clinical Oncology Group Study 9104*. J Clin Oncol, 2002. **20**(14): p. 3054-60.
8. Dubin, S. and D. Griffin, *Lung Cancer in Non-Smokers*. Mo Med, 2020. **117**(4): p. 375-379.
9. Chheang, S. and K. Brown, *Lung cancer staging: clinical and radiologic perspectives*. Semin Intervent Radiol, 2013. **30**(2): p. 99-113.
10. Marushima, H., et al., *Survival outcomes of adjuvant chemotherapy with modified weekly nab-paclitaxel and carboplatin for completely resected nonsmall cell lung cancer: FAST-nab*. Anticancer Drugs, 2020. **31**(2): p. 177-182.
11. Pignon, J.P., et al., *Lung adjuvant cisplatin evaluation: a pooled analysis by the LACE Collaborative Group*. J Clin Oncol, 2008. **26**(21): p. 3552-9.
12. Molina, J.R., et al., *Non-small cell lung cancer: epidemiology, risk factors, treatment, and survivorship*. Mayo Clin Proc, 2008. **83**(5): p. 584-94.
13. Scagliotti, G.V., et al., *Phase III randomized trial comparing three platinum-based doublets in advanced non-small-cell lung cancer*. J Clin Oncol, 2002. **20**(21): p. 4285-91.
14. Manegold, C., *Chemotherapy for advanced non-small cell lung cancer: standards*. Lung Cancer, 2001. **34 Suppl 2**: p. S165-70.
15. Lynch, T.J., et al., *Activating mutations in the epidermal growth factor receptor underlying responsiveness of non-small-cell lung cancer to gefitinib*. N Engl J Med, 2004. **350**(21): p. 2129-39.
16. Miyauchi, E., et al., *Efficacy of chemotherapy after first-line gefitinib therapy in EGFR mutation-positive advanced non-small cell lung cancer-data from a randomized Phase III study comparing gefitinib with carboplatin plus paclitaxel (NEJ002)*. Jpn J Clin Oncol, 2015. **45**(7): p. 670-6.
17. Inoue, A., et al., *Updated overall survival results from a randomized phase III trial comparing gefitinib with carboplatin-paclitaxel for chemo-naive non-small cell lung cancer with sensitive EGFR gene mutations (NEJ002)*. Ann Oncol, 2013. **24**(1): p. 54-9.
18. Fukuoka, M., et al., *Biomarker analyses and final overall survival results from a phase III, randomized, open-label, first-line study of gefitinib versus carboplatin/paclitaxel in clinically selected patients with advanced non-small-cell lung cancer in Asia (IPASS)*. J Clin Oncol, 2011. **29**(21): p. 2866-74.
19. Mok, T.S., et al., *Gefitinib or carboplatin-paclitaxel in pulmonary adenocarcinoma*. N Engl J Med, 2009. **361**(10): p. 947-57.
20. Fearon, E.R. and B. Vogelstein, *A genetic model for colorectal tumorigenesis*. Cell, 1990. **61**(5): p. 759-67.
21. Vogelstein, B., et al., *Genetic alterations during colorectal-tumor development*. N Engl J Med, 1988. **319**(9): p. 525-32.

22. Planchard, D., et al., *Metastatic non-small cell lung cancer: ESMO Clinical Practice Guidelines for diagnosis, treatment and follow-up*. Ann Oncol, 2018. **29**(Suppl 4): p. iv192-iv237.
23. Hashim, D., et al., *The global decrease in cancer mortality: trends and disparities*. Ann Oncol, 2016. **27**(5): p. 926-33.
24. Li, W., et al., *Genetic variants of DNA repair pathway genes on lung cancer risk*. Pathol Res Pract, 2019. **215**(10): p. 152548.
25. Kiyohara, C., K. Takayama, and Y. Nakanishi, *Lung cancer risk and genetic polymorphisms in DNA repair pathways: a meta-analysis*. J Nucleic Acids, 2010. **2010**: p. 701760.
26. Rizvi, N.A., et al., *Cancer immunology. Mutational landscape determines sensitivity to PD-1 blockade in non-small cell lung cancer*. Science, 2015. **348**(6230): p. 124-8.
27. Campbell, J.D., et al., *Distinct patterns of somatic genome alterations in lung adenocarcinomas and squamous cell carcinomas*. Nat Genet, 2016. **48**(6): p. 607-16.
28. Kris, M.G., et al., *Using multiplexed assays of oncogenic drivers in lung cancers to select targeted drugs*. JAMA, 2014. **311**(19): p. 1998-2006.
29. Imyanitov, E.N., A.G. Iyevleva, and E.V. Levchenko, *Molecular testing and targeted therapy for non-small cell lung cancer: Current status and perspectives*. Crit Rev Oncol Hematol, 2021. **157**: p. 103194.
30. Gagan, J. and E.M. Van Allen, *Next-generation sequencing to guide cancer therapy*. Genome Med, 2015. **7**(1): p. 80.
31. Wu, K., et al., *Next-generation sequencing for lung cancer*. Future Oncol, 2013. **9**(9): p. 1323-36.
32. Soda, M., et al., *Identification of the transforming EML4-ALK fusion gene in non-small-cell lung cancer*. Nature, 2007. **448**(7153): p. 561-6.
33. Rikova, K., et al., *Global survey of phosphotyrosine signaling identifies oncogenic kinases in lung cancer*. Cell, 2007. **131**(6): p. 1190-203.
34. Marchetti, A., et al., *Clinical features and outcome of patients with non-small-cell lung cancer harboring BRAF mutations*. J Clin Oncol, 2011. **29**(26): p. 3574-9.
35. Naoki, K., et al., *Missense mutations of the BRAF gene in human lung adenocarcinoma*. Cancer Res, 2002. **62**(23): p. 7001-3.
36. Sequist, L.V., et al., *Implementing multiplexed genotyping of non-small-cell lung cancers into routine clinical practice*. Ann Oncol, 2011. **22**(12): p. 2616-2624.
37. Wang, R., et al., *RET fusions define a unique molecular and clinicopathologic subtype of non-small-cell lung cancer*. J Clin Oncol, 2012. **30**(35): p. 4352-9.
38. Seo, J.S., et al., *The transcriptional landscape and mutational profile of lung adenocarcinoma*. Genome Res, 2012. **22**(11): p. 2109-19.
39. Beau-Faller, M., et al., *MET gene copy number in non-small cell lung cancer: molecular analysis in a targeted tyrosine kinase inhibitor naive cohort*. J Thorac Oncol, 2008. **3**(4): p. 331-9.
40. Cocco, E., M. Scaltriti, and A. Drilon, *NTRK fusion-positive cancers and TRK inhibitor therapy*. Nat Rev Clin Oncol, 2018. **15**(12): p. 731-747.
41. Farago, A.F., et al., *Clinicopathologic Features of Non-Small-Cell Lung Cancer Harboring an NTRK Gene Fusion*. JCO Precis Oncol, 2018. **2018**.
42. Hirsch, F.R., et al., *Evaluation of HER-2/neu gene amplification and protein expression in non-small cell lung carcinomas*. Br J Cancer, 2002. **86**(9): p. 1449-56.
43. Facchinetti, F., et al., *LKB1/STK11 mutations in non-small cell lung cancer patients: Descriptive analysis and prognostic value*. Lung Cancer, 2017. **112**: p. 62-68.
44. Laderian, B., et al., *Emerging Therapeutic Implications of STK11 Mutation: Case Series*. Oncologist, 2020. **25**(9): p. 733-737.
45. Nadal, E., R. Palmero, and C. Munoz-Pinedo, *Mutations in the Antioxidant KEAP1/NRF2 Pathway Define an Aggressive Subset of NSCLC Resistant to Conventional Treatments*. J Thorac Oncol, 2019. **14**(11): p. 1881-1883.
46. Prall, O.W.J., et al., *Mutations in TP53 and other heterogeneous genes help to distinguish metastases from new primary malignancies*. medRxiv, 2020: p. 2020.11.11.20226845.
47. Devarakonda, S., D. Morgensztern, and R. Govindan, *Genomic alterations in lung*

- adenocarcinoma. *Lancet Oncol*, 2015. **16**(7): p. e342-51.
48. Li, Y., et al., *Clinical significance of EML4-ALK fusion gene and association with EGFR and KRAS gene mutations in 208 Chinese patients with non-small cell lung cancer*. *PLoS One*, 2013. **8**(1): p. e52093.
49. Koh, Y., et al., *Clinicopathologic characteristics and outcomes of patients with anaplastic lymphoma kinase-positive advanced pulmonary adenocarcinoma: suggestion for an effective screening strategy for these tumors*. *J Thorac Oncol*, 2011. **6**(5): p. 905-12.
50. Riely, G.J., et al., *Frequency and distinctive spectrum of KRAS mutations in never smokers with lung adenocarcinoma*. *Clin Cancer Res*, 2008. **14**(18): p. 5731-4.
51. Kim, T.J., et al., *Simultaneous diagnostic platform of genotyping EGFR, KRAS, and ALK in 510 Korean patients with non-small-cell lung cancer highlights significantly higher ALK rearrangement rate in advanced stage*. *J Surg Oncol*, 2014. **110**(3): p. 245-51.
52. Morris, S.W., et al., *ALK, the chromosome 2 gene locus altered by the t(2;5) in non-Hodgkin's lymphoma, encodes a novel neural receptor tyrosine kinase that is highly related to leukocyte tyrosine kinase (LTK)*. *Oncogene*, 1997. **14**(18): p. 2175-88.
53. Alonso, A., et al., *Protein tyrosine phosphatases in the human genome*. *Cell*, 2004. **117**(6): p. 699-711.
54. Manning, G., et al., *The protein kinase complement of the human genome*. *Science*, 2002. **298**(5600): p. 1912-34.
55. Reshetnyak, A.V., et al., *Augmentor alpha and beta (FAM150) are ligands of the receptor tyrosine kinases ALK and LTK: Hierarchy and specificity of ligand-receptor interactions*. *Proc Natl Acad Sci U S A*, 2015. **112**(52): p. 15862-7.
56. Shaw, A.T. and B. Solomon, *Targeting anaplastic lymphoma kinase in lung cancer*. *Clin Cancer Res*, 2011. **17**(8): p. 2081-6.
57. Webb, T.R., et al., *Anaplastic lymphoma kinase: role in cancer pathogenesis and small-molecule inhibitor development for therapy*. *Expert Rev Anticancer Ther*, 2009. **9**(3): p. 331-56.
58. Roskoski, R., Jr., *Anaplastic lymphoma kinase (ALK): structure, oncogenic activation, and pharmacological inhibition*. *Pharmacol Res*, 2013. **68**(1): p. 68-94.
59. Hallberg, B. and R.H. Palmer, *The role of the ALK receptor in cancer biology*. *Ann Oncol*, 2016. **27 Suppl 3**: p. iii4-iii15.
60. Bhullar, K.S., et al., *Kinase-targeted cancer therapies: progress, challenges and future directions*. *Mol Cancer*, 2018. **17**(1): p. 48.
61. Le, T. and D.E. Gerber, *ALK alterations and inhibition in lung cancer*. *Semin Cancer Biol*, 2017. **42**: p. 81-88.
62. Sabir, S.R., et al., *EML4-ALK Variants: Biological and Molecular Properties, and the Implications for Patients*. *Cancers (Basel)*, 2017. **9**(9).
63. Adib, R., et al., *Mitotic phosphorylation by NEK6 and NEK7 reduces the microtubule affinity of EML4 to promote chromosome congression*. *Sci Signal*, 2019. **12**(594).
64. Pollmann, M., et al., *Human EML4, a novel member of the EMAP family, is essential for microtubule formation*. *Exp Cell Res*, 2006. **312**(17): p. 3241-51.
65. Chen, D., et al., *EML4 promotes the loading of NUDC to the spindle for mitotic progression*. *Cell Cycle*, 2015. **14**(10): p. 1529-39.
66. Choi, Y.L., et al., *Identification of novel isoforms of the EML4-ALK transforming gene in non-small cell lung cancer*. *Cancer Res*, 2008. **68**(13): p. 4971-6.
67. Sanders, H.R., et al., *Exon scanning by reverse transcriptase-polymerase chain reaction for detection of known and novel EML4-ALK fusion variants in non-small cell lung cancer*. *Cancer Genet*, 2011. **204**(1): p. 45-52.
68. Woo, C.G., et al., *Differential protein stability and clinical responses of EML4-ALK fusion variants to various ALK inhibitors in advanced ALK-rearranged non-small cell lung cancer*. *Ann Oncol*, 2017. **28**(4): p. 791-797.
69. Soda, M., et al., *A prospective PCR-based screening for the EML4-ALK oncogene in non-small cell lung cancer*. *Clin Cancer Res*, 2012. **18**(20): p. 5682-9.
70. Choi, Y.L., et al., *EML4-ALK mutations in lung cancer that confer resistance to ALK inhibitors*. *N Engl J Med*, 2010. **363**(18): p. 1734-9.
71. Sasaki, T., et al., *The biology and treatment of EML4-ALK non-small cell lung cancer*.

- Eur J Cancer, 2010. **46**(10): p. 1773-80.
72. Bayliss, R., et al., *Molecular mechanisms that underpin EML4-ALK driven cancers and their response to targeted drugs*. Cell Mol Life Sci, 2016. **73**(6): p. 1209-24.
73. Lovly, C.M., et al., *Rationale for co-targeting IGF-1R and ALK in ALK fusion-positive lung cancer*. Nat Med, 2014. **20**(9): p. 1027-34.
74. Koivunen, J.P., et al., *EML4-ALK fusion gene and efficacy of an ALK kinase inhibitor in lung cancer*. Clin Cancer Res, 2008. **14**(13): p. 4275-83.
75. Takeuchi, K., et al., *Multiplex reverse transcription-PCR screening for EML4-ALK fusion transcripts*. Clin Cancer Res, 2008. **14**(20): p. 6618-24.
76. Wong, D.W., et al., *The EML4-ALK fusion gene is involved in various histologic types of lung cancers from nonsmokers with wild-type EGFR and KRAS*. Cancer, 2009. **115**(8): p. 1723-33.
77. Takeuchi, K., et al., *KIF5B-ALK, a novel fusion oncokinase identified by an immunohistochemistry-based diagnostic system for ALK-positive lung cancer*. Clin Cancer Res, 2009. **15**(9): p. 3143-9.
78. Gainor, J.F., et al., *Molecular Mechanisms of Resistance to First- and Second-Generation ALK Inhibitors in ALK-Rearranged Lung Cancer*. Cancer Discov, 2016. **6**(10): p. 1118-1133.
79. Shaw, A.T., et al., *Crizotinib versus chemotherapy in advanced ALK-positive lung cancer*. N Engl J Med, 2013. **368**(25): p. 2385-94.
80. Solomon, B.J., et al., *First-line crizotinib versus chemotherapy in ALK-positive lung cancer*. N Engl J Med, 2014. **371**(23): p. 2167-77.
81. Soria, J.C., et al., *First-line ceritinib versus platinum-based chemotherapy in advanced ALK-rearranged non-small-cell lung cancer (ASCEND-4): a randomised, open-label, phase 3 study*. Lancet, 2017. **389**(10072): p. 917-929.
82. Hari, S.B., E.A. Merritt, and D.J. Maly, *Conformation-selective ATP-competitive inhibitors control regulatory interactions and noncatalytic functions of mitogen-activated protein kinases*. Chem Biol, 2014. **21**(5): p. 628-35.
83. Garuti, L., M. Roberti, and G. Bottegoni, *Non-ATP competitive protein kinase inhibitors*. Curr Med Chem, 2010. **17**(25): p. 2804-21.
84. Drilon, A., et al., *Safety and Antitumor Activity of the Multitargeted Pan-TRK, ROS1, and ALK Inhibitor Entrectinib: Combined Results from Two Phase I Trials (ALKA-372-001 and STARTRK-1)*. Cancer Discov, 2017. **7**(4): p. 400-409.
85. Roskoski, R., Jr., *Anaplastic lymphoma kinase (ALK) inhibitors in the treatment of ALK-driven lung cancers*. Pharmacol Res, 2017. **117**: p. 343-356.
86. Kwak, E.L., et al., *Anaplastic lymphoma kinase inhibition in non-small-cell lung cancer*. N Engl J Med, 2010. **363**(18): p. 1693-703.
87. Blackhall, F., et al., *Final results of the large-scale multinational trial PROFILE 1005: efficacy and safety of crizotinib in previously treated patients with advanced/metastatic ALK-positive non-small-cell lung cancer*. ESMO Open, 2017. **2**(3): p. e000219.
88. Camidge, D.R., et al., *Activity and safety of crizotinib in patients with ALK-positive non-small-cell lung cancer: updated results from a phase 1 study*. Lancet Oncol, 2012. **13**(10): p. 1011-9.
89. Shaw, A.T. and J.A. Engelman, *Ceritinib in ALK-rearranged non-small-cell lung cancer*. N Engl J Med, 2014. **370**(26): p. 2537-9.
90. Kim, D.W., et al., *Activity and safety of ceritinib in patients with ALK-rearranged non-small-cell lung cancer (ASCEND-1): updated results from the multicentre, open-label, phase 1 trial*. Lancet Oncol, 2016. **17**(4): p. 452-463.
91. Crino, L., et al., *Multicenter Phase II Study of Whole-Body and Intracranial Activity With Ceritinib in Patients With ALK-Rearranged Non-Small-Cell Lung Cancer Previously Treated With Chemotherapy and Crizotinib: Results From ASCEND-2*. J Clin Oncol, 2016. **34**(24): p. 2866-73.
92. Khan, M., et al., *ALK Inhibitors in the Treatment of ALK Positive NSCLC*. Front Oncol, 2018. **8**: p. 557.
93. Kinoshita, K., et al., *Design and synthesis of a highly selective, orally active and potent anaplastic lymphoma kinase inhibitor (CH5424802)*. Bioorg Med Chem, 2012. **20**(3): p. 1271-80.

94. Sakamoto, H., et al., *CH5424802, a selective ALK inhibitor capable of blocking the resistant gatekeeper mutant*. *Cancer Cell*, 2011. **19**(5): p. 679-90.
95. Shaw, A.T., et al., *Alectinib in ALK-positive, crizotinib-resistant, non-small-cell lung cancer: a single-group, multicentre, phase 2 trial*. *Lancet Oncol*, 2016. **17**(2): p. 234-242.
96. Seto, T., et al., *CH5424802 (RO5424802) for patients with ALK-rearranged advanced non-small-cell lung cancer (AF-001JP study): a single-arm, open-label, phase 1-2 study*. *Lancet Oncol*, 2013. **14**(7): p. 590-8.
97. Peters, S., et al., *Alectinib versus Crizotinib in Untreated ALK-Positive Non-Small-Cell Lung Cancer*. *N Engl J Med*, 2017. **377**(9): p. 829-838.
98. Markham, A., *Brigatinib: First Global Approval*. *Drugs*, 2017. **77**(10): p. 1131-1135.
99. Zhang, S., et al., *The Potent ALK Inhibitor Brigatinib (AP26113) Overcomes Mechanisms of Resistance to First- and Second-Generation ALK Inhibitors in Preclinical Models*. *Clin Cancer Res*, 2016. **22**(22): p. 5527-5538.
100. Huber, R.M., et al., *Brigatinib in Crizotinib-Refractory ALK+ NSCLC: 2-Year Follow-up on Systemic and Intracranial Outcomes in the Phase 2 ALTA Trial*. *J Thorac Oncol*, 2020. **15**(3): p. 404-415.
101. Kim, D.W., et al., *Brigatinib in Patients With Crizotinib-Refractory Anaplastic Lymphoma Kinase-Positive Non-Small-Cell Lung Cancer: A Randomized, Multicenter Phase II Trial*. *J Clin Oncol*, 2017. **35**(22): p. 2490-2498.
102. Camidge, D.R., et al., *Brigatinib Versus Crizotinib in Advanced ALK Inhibitor-Naive ALK-Positive Non-Small Cell Lung Cancer: Second Interim Analysis of the Phase III ALTA-1L Trial*. *J Clin Oncol*, 2020. **38**(31): p. 3592-3603.
103. Friedlaender, A., et al., *Diagnosis and Treatment of ALK Aberrations in Metastatic NSCLC*. *Curr Treat Options Oncol*, 2019. **20**(10): p. 79.
104. El Darsa, H., O. Abdel-Rahman, and R. Sangha, *Pharmacological and clinical properties of lorlatinib in the treatment of ALK-rearranged advanced non-small cell lung cancer*. *Expert Opin Pharmacother*, 2020. **21**(13): p. 1547-1554.
105. Solomon, B.J., et al., *Lorlatinib in patients with ALK-positive non-small-cell lung cancer: results from a global phase 2 study*. *Lancet Oncol*, 2018. **19**(12): p. 1654-1667.
106. Shaw, A.T., et al., *ALK Resistance Mutations and Efficacy of Lorlatinib in Advanced Anaplastic Lymphoma Kinase-Positive Non-Small-Cell Lung Cancer*. *J Clin Oncol*, 2019. **37**(16): p. 1370-1379.
107. Patel, M.R., et al., *STARTRK-1: Phase 1/2a study of entrectinib, an oral Pan-Trk, ROS1, and ALK inhibitor, in patients with advanced solid tumors with relevant molecular alterations*. *Journal of Clinical Oncology*, 2015. **33**(15_suppl): p. 2596-2596.
108. Lovly, C.M., et al., *Insights into ALK-driven cancers revealed through development of novel ALK tyrosine kinase inhibitors*. *Cancer Res*, 2011. **71**(14): p. 4920-31.
109. Horn, L., et al., *Ensartinib (X-396) in ALK-Positive Non-Small Cell Lung Cancer: Results from a First-in-Human Phase I/II, Multicenter Study*. *Clin Cancer Res*, 2018. **24**(12): p. 2771-2779.
110. Yang, Y., et al., *Efficacy, safety, and biomarker analysis of ensartinib in crizotinib-resistant, ALK-positive non-small-cell lung cancer: a multicentre, phase 2 trial*. *Lancet Respir Med*, 2020. **8**(1): p. 45-53.
111. Horn, L., et al., *eXalt3: Phase III randomized study comparing ensartinib to crizotinib in anaplastic lymphoma kinase positive non-small cell lung cancer patients*. *Annals of Oncology*, 2018. **29**: p. viii543.
112. Weiss, G.J., et al., *Phase (Ph) 1/2 study of TSR-011, a potent inhibitor of ALK and TRK, including crizotinib-resistant ALK mutations*. *Journal of Clinical Oncology*, 2014. **32**(15_suppl): p. e19005-e19005.
113. Lin, C.C., et al., *A phase 1, open-label, dose-escalation trial of oral TSR-011 in patients with advanced solid tumours and lymphomas*. *Br J Cancer*, 2019. **121**(2): p. 131-138.
114. Ott, G.R., et al., *Discovery of Clinical Candidate CEP-37440, a Selective Inhibitor of Focal Adhesion Kinase (FAK) and Anaplastic Lymphoma Kinase (ALK)*. *J Med Chem*, 2016. **59**(16): p. 7478-96.

115. Kiura, K., et al., *Phase 3 study of ceritinib vs chemotherapy in ALK-rearranged NSCLC patients previously treated with chemotherapy and crizotinib (ASCEND-5): Japanese subset*. Jpn J Clin Oncol, 2018. **48**(4): p. 367-375.
116. Shaw, A.T., et al., *Ceritinib versus chemotherapy in patients with ALK-rearranged non-small-cell lung cancer previously given chemotherapy and crizotinib (ASCEND-5): a randomised, controlled, open-label, phase 3 trial*. Lancet Oncol, 2017. **18**(7): p. 874-886.
117. Hida, T., et al., *Alectinib versus crizotinib in patients with ALK-positive non-small-cell lung cancer (J-ALEX): an open-label, randomised phase 3 trial*. Lancet, 2017. **390**(10089): p. 29-39.
118. Gadgeel, S.M., et al., *Safety and activity of alectinib against systemic disease and brain metastases in patients with crizotinib-resistant ALK-rearranged non-small-cell lung cancer (AF-002JG): results from the dose-finding portion of a phase 1/2 study*. Lancet Oncol, 2014. **15**(10): p. 1119-28.
119. Johnson, T.W., et al., *Discovery of (10R)-7-amino-12-fluoro-2,10,16-trimethyl-15-oxo-10,15,16,17-tetrahydro-2H-8,4-(m etheno)pyrazolo[4,3-h][2,5,11]-benzoxadiazacyclotetradecine-3-carbonitrile (PF-06463922), a macrocyclic inhibitor of anaplastic lymphoma kinase (ALK) and c-ros oncogene 1 (ROS1) with preclinical brain exposure and broad-spectrum potency against ALK-resistant mutations*. J Med Chem, 2014. **57**(11): p. 4720-44.
120. Liu, N., et al., *A case of primary pulmonary atypical carcinoid with EML4-ALK rearrangement*. Cancer Biol Ther, 2020. **21**(1): p. 12-16.
121. Huang, W.S., et al., *Discovery of Brigatinib (AP26113), a Phosphine Oxide-Containing, Potent, Orally Active Inhibitor of Anaplastic Lymphoma Kinase*. J Med Chem, 2016. **59**(10): p. 4948-64.
122. Fontana, D., et al., *Activity of second-generation ALK inhibitors against crizotinib-resistant mutants in an NPM-ALK model compared to EML4-ALK*. Cancer Med, 2015. **4**(7): p. 953-65.
123. Zou, H.Y., et al., *PF-06463922 is a potent and selective next-generation ROS1/ALK inhibitor capable of blocking crizotinib-resistant ROS1 mutations*. Proc Natl Acad Sci U S A, 2015. **112**(11): p. 3493-8.
124. Ardini, E., et al., *Entrectinib, a Pan-TRK, ROS1, and ALK Inhibitor with Activity in Multiple Molecularly Defined Cancer Indications*. Mol Cancer Ther, 2016. **15**(4): p. 628-39.
125. Salem, I., et al., *The effects of CEP-37440, an inhibitor of focal adhesion kinase, in vitro and in vivo on inflammatory breast cancer cells*. Breast Cancer Res, 2016. **18**(1): p. 37.
126. Miyawaki, M., et al., *Overcoming EGFR Bypass Signal-Induced Acquired Resistance to ALK Tyrosine Kinase Inhibitors in ALK-Translocated Lung Cancer*. Mol Cancer Res, 2017. **15**(1): p. 106-114.
127. Sasaki, T., et al., *A novel ALK secondary mutation and EGFR signaling cause resistance to ALK kinase inhibitors*. Cancer Res, 2011. **71**(18): p. 6051-60.
128. Wilson, F.H., et al., *A functional landscape of resistance to ALK inhibition in lung cancer*. Cancer Cell, 2015. **27**(3): p. 397-408.
129. Gouji, T., et al., *Crizotinib can overcome acquired resistance to CH5424802: is amplification of the MET gene a key factor?* J Thorac Oncol, 2014. **9**(3): p. e27-8.
130. Crystal, A.S., et al., *Patient-derived models of acquired resistance can identify effective drug combinations for cancer*. Science, 2014. **346**(6216): p. 1480-6.
131. Gower, A., et al., *EMT is associated with, but does not drive resistance to ALK inhibitors among EML4-ALK non-small cell lung cancer*. Mol Oncol, 2016. **10**(4): p. 601-9.
132. Kim, H.R., et al., *Epithelial-mesenchymal transition leads to crizotinib resistance in H2228 lung cancer cells with EML4-ALK translocation*. Mol Oncol, 2013. **7**(6): p. 1093-102.
133. Heuckmann, J.M., et al., *Differential protein stability and ALK inhibitor sensitivity of EML4-ALK fusion variants*. Clin Cancer Res, 2012. **18**(17): p. 4682-90.
134. Christopoulos, P., et al., *EML4-ALK fusion variant V3 is a high-risk feature conferring accelerated metastatic spread, early treatment failure and worse overall survival in*

- ALK(+) non-small cell lung cancer*. *Int J Cancer*, 2018. **142**(12): p. 2589-2598.
135. Mitiushkina, N.V., et al., *Variability in lung cancer response to ALK inhibitors cannot be explained by the diversity of ALK fusion variants*. *Biochimie*, 2018. **154**: p. 19-24.
136. Lei, Y.Y., et al., *Anaplastic Lymphoma Kinase Variants and the Percentage of ALK-Positive Tumor Cells and the Efficacy of Crizotinib in Advanced NSCLC*. *Clin Lung Cancer*, 2016. **17**(3): p. 223-31.
137. Cha, Y.J., H.R. Kim, and H.S. Shim, *Clinical outcomes in ALK-rearranged lung adenocarcinomas according to ALK fusion variants*. *J Transl Med*, 2016. **14**(1): p. 296.
138. Taylor, S.S. and A.P. Kornev, *Protein kinases: evolution of dynamic regulatory proteins*. *Trends Biochem Sci*, 2011. **36**(2): p. 65-77.
139. Friboulet, L., et al., *The ALK inhibitor ceritinib overcomes crizotinib resistance in non-small cell lung cancer*. *Cancer Discov*, 2014. **4**(6): p. 662-673.
140. Katayama, R., et al., *Mechanisms of acquired crizotinib resistance in ALK-rearranged lung Cancers*. *Sci Transl Med*, 2012. **4**(120): p. 120ra17.
141. Katayama, R., et al., *Two novel ALK mutations mediate acquired resistance to the next-generation ALK inhibitor alectinib*. *Clin Cancer Res*, 2014. **20**(22): p. 5686-96.
142. Zhang, J., P.L. Yang, and N.S. Gray, *Targeting cancer with small molecule kinase inhibitors*. *Nat Rev Cancer*, 2009. **9**(1): p. 28-39.
143. Ignatius Ou, S.H., et al., *Next-generation sequencing reveals a Novel NSCLC ALK F1174V mutation and confirms ALK G1202R mutation confers high-level resistance to alectinib (CH5424802/RO5424802) in ALK-rearranged NSCLC patients who progressed on crizotinib*. *J Thorac Oncol*, 2014. **9**(4): p. 549-53.
144. Kornev, A.P., et al., *Surface comparison of active and inactive protein kinases identifies a conserved activation mechanism*. *Proc Natl Acad Sci U S A*, 2006. **103**(47): p. 17783-8.
145. Katayama, R., et al., *Therapeutic strategies to overcome crizotinib resistance in non-small cell lung cancers harboring the fusion oncogene EML4-ALK*. *Proc Natl Acad Sci U S A*, 2011. **108**(18): p. 7535-40.
146. Lin, J.J., G.J. Riely, and A.T. Shaw, *Targeting ALK: Precision Medicine Takes on Drug Resistance*. *Cancer Discov*, 2017. **7**(2): p. 137-155.
147. Massarelli, E. and V. Papadimitrakopoulou, *Ceritinib for the treatment of late-stage (metastatic) non-small cell lung cancer*. *Clin Cancer Res*, 2015. **21**(4): p. 670-4.
148. Noe, J., et al., *ALK Mutation Status Before and After Alectinib Treatment in Locally Advanced or Metastatic ALK-Positive NSCLC: Pooled Analysis of Two Prospective Trials*. *J Thorac Oncol*, 2020. **15**(4): p. 601-608.
149. Shaw, A.T., et al., *Resensitization to Crizotinib by the Lorlatinib ALK Resistance Mutation L1198F*. *N Engl J Med*, 2016. **374**(1): p. 54-61.
150. Koopman, B., et al., *Actionability of on-target ALK Resistance Mutations in Patients With Non-Small Cell Lung Cancer: Local Experience and Review of the Literature*. *Clin Lung Cancer*, 2021.
151. Patterson, S.E., et al., *The clinical trial landscape in oncology and connectivity of somatic mutational profiles to targeted therapies*. *Hum Genomics*, 2016. **10**: p. 4.
152. Griffith, M., et al., *CIViC is a community knowledgebase for expert crowdsourcing the clinical interpretation of variants in cancer*. *Nat Genet*, 2017. **49**(2): p. 170-174.
153. Wang, M., *Fusion of EML4-ALK Variant is associated with Differential Response to targeted ALK Kinase Inhibitors in Non-Small Cell Lung Cancer (NSCLC)*. Dr. Med thesis (in preparation), 2021.
154. Towbin, H., T. Staehelin, and J. Gordon, *Electrophoretic transfer of proteins from polyacrylamide gels to nitrocellulose sheets: procedure and some applications*. *Proc Natl Acad Sci U S A*, 1979. **76**(9): p. 4350-4.
155. Trott, O. and A.J. Olson, *AutoDock Vina: improving the speed and accuracy of docking with a new scoring function, efficient optimization, and multithreading*. *J Comput Chem*, 2010. **31**(2): p. 455-61.
156. Morris, G.M., et al., *AutoDock4 and AutoDockTools4: Automated docking with selective receptor flexibility*. *J Comput Chem*, 2009. **30**(16): p. 2785-91.
157. Huey, R., et al., *A semiempirical free energy force field with charge-based desolvation*. *J Comput Chem*, 2007. **28**(6): p. 1145-52.

158. *The PyMOL Molecular Graphics System, Version 1.2r3pre, Schrödinger, LLC.*
159. Papachristou, D.J., et al., *Expression of integrin-linked kinase and its binding partners in chondrosarcoma: association with prognostic significance.* Eur J Cancer, 2008. **44**(16): p. 2518-25.
160. Choi, Y.L., et al., *EML4-ALK Mutations in Lung Cancer That Confer Resistance to ALK Inhibitors.* The New England Journal of Medicine, 2010(363): p. 1734-9.
161. Recondo, G., et al., *Diverse Resistance Mechanisms to the Third-Generation ALK Inhibitor Lorlatinib in ALK-Rearranged Lung Cancer.* Clin Cancer Res, 2020. **26**(1): p. 242-255.
162. Wang, H.Y., C.C. Ho, and J.Y. Shih, *Multiple Acquired Resistance Mutations of the ALK Tyrosine Kinase Domain after Sequential Use of ALK Inhibitors.* J Thorac Oncol, 2017. **12**(5): p. e49-e51.
163. Ding, M., et al., *Case Report: Temporal Heterogeneity of ALK Activating Mutations in Sequential ALK TKI-Treated Non-Small-Cell Lung Cancer Revealed Using NGS-Based Liquid Biopsy.* Clin Lung Cancer, 2019. **20**(3): p. e229-e232.
164. Doebele, R.C., et al., *Mechanisms of resistance to crizotinib in patients with ALK gene rearranged non-small cell lung cancer.* Clin Cancer Res, 2012. **18**(5): p. 1472-82.
165. Toyokawa, G., et al., *Secondary mutations at I1171 in the ALK gene confer resistance to both Crizotinib and Alectinib.* J Thorac Oncol, 2014. **9**(12): p. e86-7.
166. Horn, L., et al., *Monitoring Therapeutic Response and Resistance: Analysis of Circulating Tumor DNA in Patients With ALK+ Lung Cancer.* J Thorac Oncol, 2019. **14**(11): p. 1901-1911.
167. Lin, J.J., et al., *Impact of EML4-ALK Variant on Resistance Mechanisms and Clinical Outcomes in ALK-Positive Lung Cancer.* J Clin Oncol, 2018. **36**(12): p. 1199-1206.
168. Varlow, C., et al., *Classics in Neuroimaging: Imaging the Endocannabinoid Pathway with PET.* ACS Chem Neurosci, 2020. **11**(13): p. 1855-1862.
169. Okada, K., et al., *Prediction of ALK mutations mediating ALK-TKIs resistance and drug re-purposing to overcome the resistance.* EBioMedicine, 2019. **41**: p. 105-119.
170. Itchins, M., et al., *ALK-Rearranged Non-Small Cell Lung Cancer in 2020: Real-World Triumphs in an Era of Multigeneration ALK-Inhibitor Sequencing Informed by Drug Resistance Profiling.* Oncologist, 2020. **25**(8): p. 641-649.
171. Palacios, R. and M. Steinmetz, *Il-3-dependent mouse clones that express B-220 surface antigen, contain Ig genes in germ-line configuration, and generate B lymphocytes in vivo.* Cell, 1985. **41**(3): p. 727-34.
172. Bordogna, A., A. Pandini, and L. Bonati, *Predicting the accuracy of protein-ligand docking on homology models.* J Comput Chem, 2011. **32**(1): p. 81-98.
173. Warmuth, M., et al., *Ba/F3 cells and their use in kinase drug discovery.* Curr Opin Oncol, 2007. **19**(1): p. 55-60.
174. Ou, S.H., et al., *Alectinib in Crizotinib-Refractory ALK-Rearranged Non-Small-Cell Lung Cancer: A Phase II Global Study.* J Clin Oncol, 2016. **34**(7): p. 661-8.
175. Shaw, A.T., et al., *Ceritinib in ALK-rearranged non-small-cell lung cancer.* N Engl J Med, 2014. **370**(13): p. 1189-97.
176. Li, B., et al., *Inhibition of neurogenic and thromboxane A2 -induced human prostate smooth muscle contraction by the integrin alpha2beta1 inhibitor BTT-3033 and the integrin-linked kinase inhibitor Cpd22.* Prostate, 2020. **80**(11): p. 831-849.
177. Ai, X., et al., *An interaction map of small-molecule kinase inhibitors with anaplastic lymphoma kinase (ALK) mutants in ALK-positive non-small cell lung cancer.* Biochimie, 2015. **112**: p. 111-20.
178. Lovly, C.M. and W. Pao, *Escaping ALK inhibition: mechanisms of and strategies to overcome resistance.* Sci Transl Med, 2012. **4**(120): p. 120ps2.
179. Sasaki, T., et al., *The neuroblastoma-associated F1174L ALK mutation causes resistance to an ALK kinase inhibitor in ALK-translocated cancers.* Cancer Res, 2010. **70**(24): p. 10038-43.
180. Kwok, H.H., et al., *Transfer of Extracellular Vesicle-Associated-RNAs Induces Drug Resistance in ALK-Translocated Lung Adenocarcinoma.* Cancers (Basel), 2019. **11**(1).
181. Katayama, R., et al., *P-glycoprotein Mediates Ceritinib Resistance in Anaplastic*

- Lymphoma Kinase-rearranged Non-small Cell Lung Cancer*. EBioMedicine, 2016. **3**: p. 54-66.
182. Yoshida, T., et al., *Differential Crizotinib Response Duration Among ALK Fusion Variants in ALK-Positive Non-Small-Cell Lung Cancer*. J Clin Oncol, 2016. **34**(28): p. 3383-9.
183. He, Y., et al., *The prevalence of EML4-ALK variants in patients with non-small-cell lung cancer: a systematic review and meta-analysis*. Biomark Med, 2019. **13**(12): p. 1035-1044.
184. Yanagitani, N., et al., *Drug resistance mechanisms in Japanese anaplastic lymphoma kinase-positive non-small cell lung cancer and the clinical responses based on the resistant mechanisms*. Cancer Sci, 2020. **111**(3): p. 932-939.
185. Takahashi, K., et al., *Overcoming resistance by ALK compound mutation (I1171S + G1269A) after sequential treatment of multiple ALK inhibitors in non-small cell lung cancer*. Thorac Cancer, 2020. **11**(3): p. 581-587.
186. Pailler, E., et al., *Acquired Resistance Mutations to ALK Inhibitors Identified by Single Circulating Tumor Cell Sequencing in ALK-Rearranged Non-Small-Cell Lung Cancer*. Clin Cancer Res, 2019. **25**(22): p. 6671-6682.
187. Dagogo-Jack, I., et al., *Treatment with Next-Generation ALK Inhibitors Fuels Plasma ALK Mutation Diversity*. Clin Cancer Res, 2019. **25**(22): p. 6662-6670.
188. Yoda, S., et al., *Sequential ALK Inhibitors Can Select for Lorlatinib-Resistant Compound ALK Mutations in ALK-Positive Lung Cancer*. Cancer Discov, 2018. **8**(6): p. 714-729.

6 Appendix A:

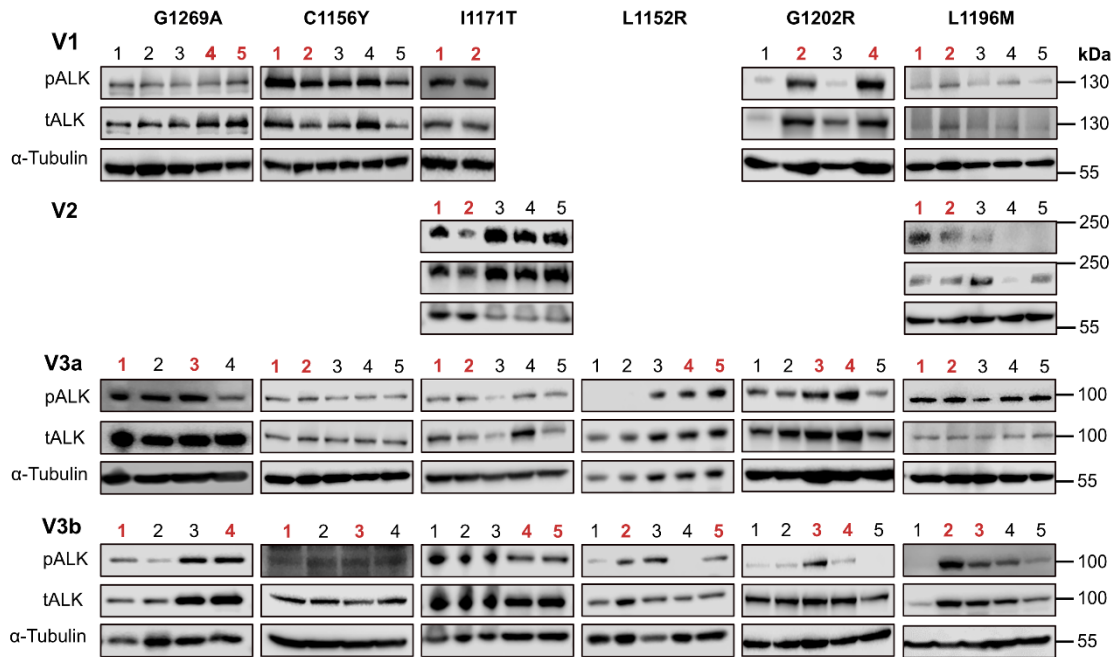


Figure Appendix A Shown are Western blots of lysates from cell clones expressing respective variants and ALK mutations. Western blot analysis was performed using antibodies for pALK, tALK and α -tubulin served as loading control. **Red bold numbers** are selected clones for subsequent drug screening.

7 Appendix B:

Table Appendix B pIC50 values of ALK-TKIs on cellular ALK phosphorylation in Ba/F3 cells harboring EML4-ALK C1156Y, L1196M, G1269A, I1171T, L1152R and G1202R mutations and corresponding variants. **Green wells and red wells** indicate absolute sensitive or resistant, respectively. **Yellow wells** indicate intermediate sensitivity or intermediate resistant. **Dark Green wells** marked the most potent inhibitors for the corresponding mutation-fusion combinant.

Mutations	Variants	Cellular mean±SD pIC50								
		CRIZ	CERT	ALEC	BRIG	LOR	BELI	ENTRE	ENSAR	CEP
C1156Y	V1	7.10±0.11	7.35±0.16	8.07±0.17	8.27±0.30	8.26±0.11	7.94±0.21	7.47±0.17	7.70±0.08	7.08±0.21
	V3a	7.19±0.10	7.32±0.14	8.23±0.23	8.42±0.16	8.72±0.29	8.18±0.45	7.72±0.20	7.89±0.14	7.31±0.13
	V3b	7.27±0.08	7.26±0.17	8.03±0.23	8.19±0.34	8.69±0.27	8.34±0.25	7.72±0.18	7.96±0.27	7.33±0.18
G1269A	V1	7.10±0.08	7.95±0.08	7.77±0.11	8.50±0.16	7.93±0.18	8.26±0.10	7.07±0.12	7.28±0.08	7.84±0.15
	V3a	7.13±0.15	7.77±0.10	7.74±0.15	8.21±0.20	7.62±0.17	8.26±0.15	6.81±0.35	7.29±0.14	7.75±0.16
	V3b	7.09±0.10	7.88±0.24	7.60±0.15	8.17±0.34	7.75±0.21	8.21±0.21	7.02±0.19	7.16±0.06	7.64±0.15
L1196M	V1	7.04±0.10	7.52±0.14	7.35±0.11	7.62±0.10	7.49±0.19	8.83±0.18	7.07±0.18	7.39±0.06	6.81±0.23
	V2	7.80±0.21	8.09±0.29	8.46±0.39	8.13±0.19	8.38±0.10	9.78±0.41	8.11±0.15	8.38±0.36	7.65±0.35
	V3a	7.04±0.05	8.19±0.39	7.78±0.27	7.90±0.19	7.91±0.11	9.21±0.22	7.46±0.15	7.54±0.24	7.20±0.17
	V3b	7.07±0.07	7.61±0.15	7.33±0.09	7.57±0.18	7.46±0.17	8.85±0.24	7.18±0.09	7.26±0.12	6.04±0.14
I1171T	V1	7.17±0.16	7.48±0.10	7.98±0.14	7.59±0.25	8.58±0.28	7.65±0.20	6.91±0.14	7.87±0.23	7.31±0.18
	V2	7.91±0.10	8.10±0.39	8.21±0.20	8.34±0.22	8.31±0.26	8.30±0.30	7.35±0.20	8.21±0.24	7.35±0.15
	V3a	7.07±0.26	7.98±0.13	7.92±0.09	8.07±0.44	8.20±0.10	8.20±0.14	7.17±0.06	8.14±0.15	7.53±0.04
	V3b	7.11±0.31	7.53±0.04	7.87±0.09	7.99±0.05	8.13±0.10	8.00±0.10	6.98±0.19	8.08±0.07	7.25±0.21
L1152R	V3a	7.11±0.11	7.22±0.35	8.18±0.34	8.72±0.23	8.33±0.37	7.74±0.31	8.08±0.28	7.82±0.39	7.35±0.10
	V3b	7.19±0.33	7.13±0.23	8.08±0.13	8.45±0.14	8.08±0.13	7.54±0.20	7.99±0.21	7.55±0.18	7.08±0.12
G1202R	V1	5.92±0.30	7.08±0.15	6.84±0.15	7.22±0.23	7.66±0.08	6.35±0.34	6.33±0.42	6.43±0.25	6.14±0.30
	V3a	5.97±0.05	6.95±0.42	6.28±0.33	6.78±0.38	7.58±0.29	6.59±0.17	5.78±0.81	6.56±0.60	6.15±0.43
	V3b	5.85±0.26	6.91±0.36	6.80±0.14	6.94±0.20	7.55±0.23	4.32±0.44	5.74±0.53	5.82±0.47	5.23±0.12

sensitive intermediate resistant

8 Acknowledgments

Prof. Andreas Jung has been an ideal teacher, mentor, and supervisor, offering advice and encouragement with a perfect blend of insight and humor. I still remember the hand-drew cute little mouse by him when I first met him and discussed the project with him on October 2rd, 2017. And I will miss our discussion time on Tuesdays, when we discussed projects like students and teachers, and discussed problems in our lives like friends. Andreas always offered me mounts of advices and inspired me. Immense gratitude as always to him for his patience and support.

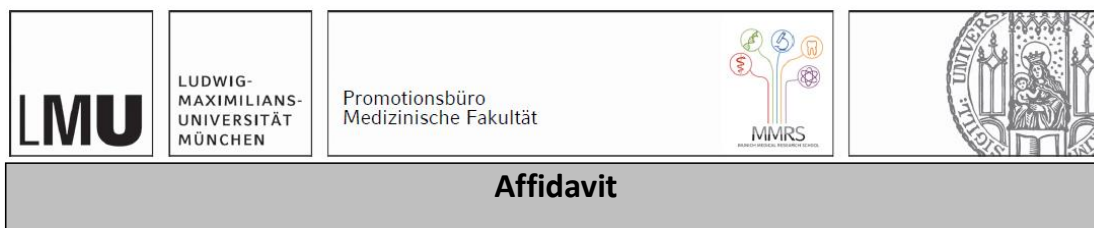
Dr. Jörg Kumbrink showed me my first cell culture here and always gave me very helpful advices on practical aspects. He also showed me by example the rigorous attitude towards scientific research. Mrs. Sabine Sagebiel had a curiosity and passion for all things and offered me tons of help throughout my projects. Meng Wang generated plasmids expressing wild type ALK gene, which were the material basis of this study. Thanks to her for always helping me when I forget how to express myself in English. This thesis builds on many ideas that were developed with their help. I am proud of, and grateful for, my time working with them.

Members of molecular diagnosis were all friendly and patient with me, and willing to help me learn what I want to learn. Other staff at the Pathology Institute made my research both productive and enjoyable. I am grateful for the cherished time spent together in the lab, and in social settings.

My special thanks goes to my parents for their endless support and continuous encouragement throughout my study. To borrow a line from Gandalf, "Home's behind, the world ahead." Without you, there is no way for me to take the adventure and thus I cannot finalize my thesis. With you, I'll discover more of my possibilities.

Finally, Bingsheng, thanks for always being there for me. You came all the way with me, shed a light on the path through the night. And I believe we will have a longer way to go, together, and uncover the sweet sunrises that await us.

9 Affidavit



Pan Li

Surname, first name

I hereby declare, that the submitted thesis entitled:

Belizatinib is a potent inhibitor for non-small cell lung cancers driven by different variants of EML4-ALK fusion proteins carrying L1196M-mutations

is my own work. I have only used the sources indicated and have not made unauthorized use of services of a third party. Where the work of others has been quoted or reproduced, the source is always given.

I further declare that the submitted thesis or parts thereof have not been presented as part of an examination degree to any other university.

Beijing, 12122022

place, date

Pan Li

Signature doctoral candidate